# CHAPTER IV

## RESULTS AND DISCUSSION

### Part A: Preparation of free-radical polymers

To obtain the desired polymers with covalently bound 4-chloro-2,5-diphenyloxazole moieties, the appropriate monomers were first synthesized. The 4-chloro-2,5-diphenyloxazole moiety can be a part of polymeric backbone as demonstrated in Case a. The synthesis leading to this polymer relies on condensation. The second method considers the chromophore as pendent to the polymeric skeleton (Case b) using free radical polymerization. PMMA was used as polymeric skeleton in Case b owing to its good physical and mechanical properties and high transparency.

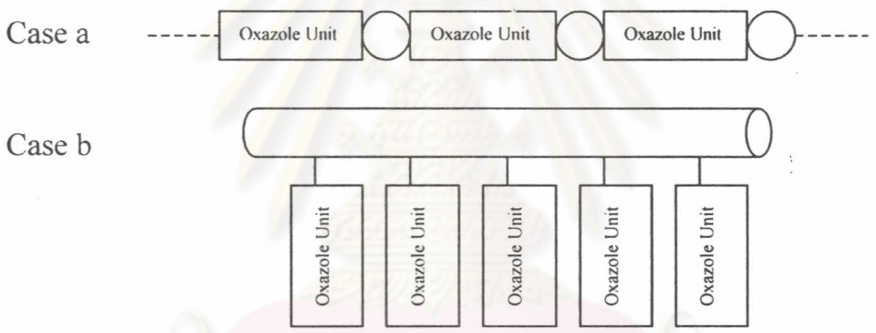


**Figure 4.1:** Design polymers containing oxazole derivatives

Two types of monomers were prepared, vinyl monomers for polymers containing 4-chloro-2,5-diphenyloxazole moieties in the side chains and di-substituted condensation monomers for construction of polymers containing 4-chloro-2,5-diphenyloxazole in the main chain. In both cases, the synthetic routes started from the corresponding benzoyl cyanide and benzadehyde.

**4.1 Synthesis of benzoyl cyanide derivatives**

Three benzoyl cyanides were synthesized from the corresponding acid chloride and cuprous cyanide. Acid chlorides react with a cyanide ion through the addition-elimination mechanism of nucleophilic acyl substitution as shown in **Scheme 4.1**. Due to the high reactivity of the acid chloride, anhydrous condition is required. Thus cuprous cyanide and acetonitrile must be dried before use.

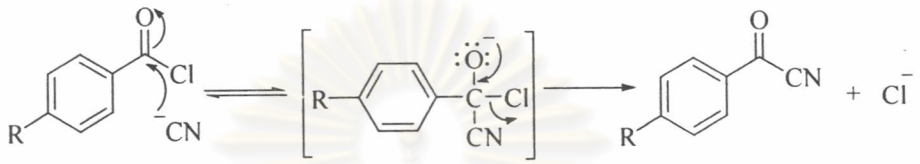

**[1a-c]**

**Scheme 4.1:** The addition-elimination mechanism of nucleophilic acyl substitution

The reactivity of the acid chloride toward nucleophilic attack depends on its structure and the attacking nucleophile. The substituents at the para position of the benzoyl chloride, thus, affected this reaction. The electron-withdrawing group, $NO_2$, enhanced the reactivity by withdrawing electron density from the carbonyl carbon via a resonance effect, creating a stronger electrophile, which was more easily attacked by the cyanide ion. Product **[1c]** was obtained in 90% yield (**Table 4.1**). Fluorine is also strongly electronegative, withdrawing electron density from a benzene ring through an inductive effect. The effect of F was slightly less than that of $NO_2$ as the yield of **[1a]** was 85%. On the other hand, the electron-donating $OCH_3$ group retarded the reactivity by donating electrons to the carbonyl carbon through a resonance effect. The yield of **[1b]** was only 50%.

**Table 4.1:** Percentage yield of benzoyl cyanide derivatives

| Compound | Substituent | % Yield |
|---|---|---|
| [1a] | F | 85 |
| [1b] | $OCH_3$ | 50 |
| [1c] | $NO_2$ | 90 |

**4-Fluorobenzoyl cyanide [1a]**: FT-IR data shows the red shift of the carbonyl absorption from 1780 $cm^{-1}$ of benzoyl chloride to about 1685 $cm^{-1}$ of benzoyl cyanide derivatives. While the disappearance of the C-Cl at 1175 $cm^{-1}$ in concomitant with the appearance of cyanide at 2222 $cm^{-1}$ was observed. The $^{1}H$ NMR spectrum of 4-fluorobenzoyl cyanide in chloroform-d exhibits the chemical shifts of aromatic protons at 8.22-8.25 and 7.31-7.35 ppm with correct integration ratios. It was clearly revealed by the appearance of the $^{13}C$ signal at 117.8 ppm, which is the characteristic signal for a nitrile carbon. The mass spectrum of this compound contained m/z peak corresponding to the calculated molecular weight of 149. The fragmentation pathway shows the loss of nitrile group (m/z = $M^{+}$-26) and phenyl radical formation (m/z = 78). The 4-fluorobenzoyl cyanide has also been analyzed by elemental analysis. The percent found elemental CHN is matched with the percent-calculated elemental composition. According to these data, it could be concluded that the product was 4-fluorobenzoyl cyanide.

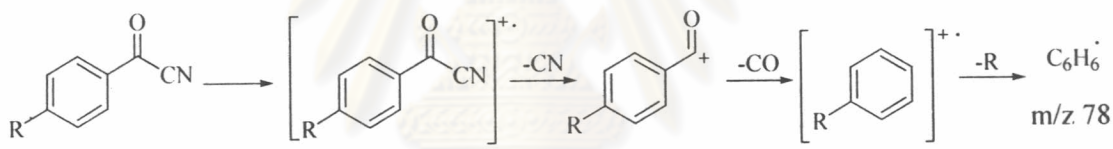


**Scheme 4.2:** Fragmentation pathway of benzoyl cyanide derivatives

**4-Methoxybenzoyl cyanide [1b]:** The spectroscopic data of this compound reveals several characteristic bands in addition to those of 4-fluorobenzoyl cyanide. From FT-IR, the carbonyl stretching is centered at 1782 $cm^{-1}$, which is higher than 4-fluorobenzoyl cyanide, 1689 $cm^{-1}$, due to resonance stabilization of the methoxy group with the phenyl ring. The 1189 $cm^{-1}$ band has been assigned to C-O-C stretch. The $^{1}H$ NMR spectrum of 4-methoxybenzoyl cyanide contains the expected features such as the C-H resonances associated with the phenyl ring between $\delta$ = 8.13-8.15 and $\delta$ = 7.07-7.09 ppm. The methoxy protons are found at $\delta$ = 3.98 ppm. The $^{13}C$ NMR spectrum reveals a characteristic nitrile signal at 114.6 ppm and methoxy signal at 56 ppm. The mass spectrum of this compound contained m/z peaks corresponding to the calculated molecular weight of 161. The percent found elemental CHN is matched

with the percent-calculated elemental composition. According to these data, it could be concluded that the product was 4-methoxybenzoyl cyanide.

**4-Nitrobenzoyl cyanide [1c]:** The spectrum of this compound reveals several characteristic bands in addition to those seen for 4-fluorobenzoyl cyanide, as noted above. From FT-IR, the 1350 $cm^{-1}$ band has been assigned to C-N stretch. The $^{1}H$ NMR spectrum of 4-nitrobenzoyl cyanide contains the down field signal of the C-H resonances associated with the phenyl ring between $\delta$ = 8.28-8.40 ppm due to deshielding effect of the nitro group. The $^{13}C$ NMR spectrum reveals a characteristic nitrile signal at 112.3 ppm. The mass spectrum of this compound contained m/z peaks corresponding to the calculated molecular weight of 176. Elemental CHN analyses indicated the presence of a nitro functionality. According to these data, it could be concluded that the product was 4-nitrobenzoyl cyanide.

**4.2 Preparation of 4-chloro-5-phenyl-2-(4′-vinylphenyl)oxazole**

After the benzoyl cyanide derivatives were obtained, the next step was to design and synthesize 4-chloro-2,5-diphenyloxazole functionalized with polymerizable groups. The design of the functionalized monomers had to fulfill a number of important criteria. The designed monomer had to function effectively as a scintillant molecule and be readily polymerized. To ensure that the designed monomers were able to scintillate, they were based upon PPO, which is a well-known scintillating molecule. It was expected that the molecule containing this oxazole moiety should retain the ability to scintillate. Two different types of PPO monomers were designed. For the first type, vinyl groups, which could be polymerized by free-radical techniques, were attached to 4-chloro-2,5-diphenyloxazoles. For the second one, 2 fluorine substituents were placed on 4-chloro-2,5-diphenyloxazole. These monomers were to be polymerized by condensation polymerization involving aromatic nucleophilic substitution of the fluorines.

The vinyl functionalized monomer, 4-chloro-5-phenyl-2-(4′-vinylphenyl) oxazole was prepared in three steps (**Scheme 4.3**) starting from benzoyl cyanide. First, benzoyl cyanide was reacted with 4-ethylbenzaldehyde in acidic condition to yield 4-chloro-2-(4′-ethylphenyl)-5-phenyloxazole **[2]**. In the next step, the 4-chloro-2-(4′-ethylphenyl)-5-phenyloxazole was treated with *N*-bromosuccinimide (NBS) in $CCl_4$ to obtain 2-[4′-(1-bromoethyl)-phenyl]-4-chloro-5-phenyloxazole **[3]**. Finally, 4-chloro-5-phenyl-2-(4′-vinylphenyl)oxazole **[4]** was obtained by dehydrobromination reaction.

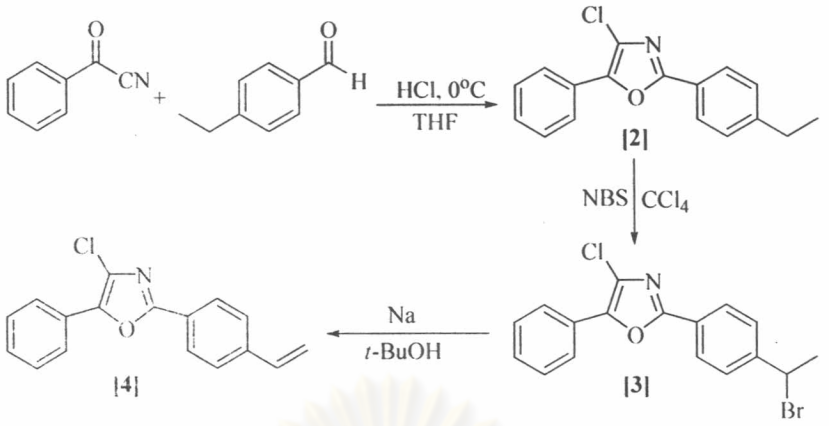


**Scheme 4.3:** Synthetic pathway of 4-chloro-5-phenyl-2-(4′-vinylphenyl)oxazole

**4-Chloro-2-(4′-ethylphenyl)-5-phenyloxazole [2]** was obtained from the cyclization reaction of benzoyl cyanide with 4-ethylbenzaldehyde in THF saturated with hydrogen chloride in one-step. The reaction yield was 65%. A possible mechanism for this cyclization reaction is shown in **Scheme 4.11**.

The FT-IR spectrum of this compound shows an absorption peak at 1580 $cm^{-1}$, which was assigned to the vibration arising from oxazole ring system. The $^{1}H$ NMR spectrum in chloroform-d exhibits the characteristic ethyl triplet at 1.24-1.29 ($J$ =7.5 Hz) ppm couple with a quartet at 2.63-2.75 ($J$ =7.5 Hz) ppm due to the $-CH_3$ and $-CH_2-$ of the ethyl group. The chemical shifts of aromatic proton appear at 7.90-8.00 (5H) and 7.50-7.30 (4H). The $^{13}C$ NMR exhibits signals of ethyl carbon at 28.8 and 15.5 ppm.

The bromination of 4-chloro-2-(4-ethylphenyl)-5-phenyloxazole was carried out by NBS/$CCl_4$ (initiated by benzoyl peroxide) to yield **2-[4′-(1-bromoethyl)-phenyl]-4-chloro-5-phenyloxazole [3]** as a yellow solid in 72% yield. The mechanism involves a chain reaction. Benzylic hydrogens are easily to remove because benzylic free radical, which is formed, is more stable owing to resonance stabilization. Thus, benzylic hydrogens can be selectively removed. The product mixtures generally do not occur.

$^1$H NMR spectrum shows the –CHBr- peak at 5.23 (q, $J$ =6.9 Hz) and a –$CH_3$ peak at 2.07 (d, $J$ =6.9 Hz) ppm. The $^{13}$C NMR exhibits signals of –$CH_3$ and –CHBr- at 26.4 and 48.2 ppm.

The **4-chloro-5-phenyl-2-(4′-vinylphenyl)oxazole [4]** was prepared by dehydrobromination reaction. $^1$H NMR of this compound showed a quartet centered at 6.74 for the –CH= and 5.86 and 5.36 ppm for the =$CH_2$ *trans* and *cis* protons, respectively. However, this Wittig reaction gave only 10% yield. The possible reason is when the size of a molecule increase, it becomes more difficult to compute mobility and relative abundance of the conformations causing low yield. Thus, this synthetic route is not appropriate to synthesize the designed monomers.

## 4.3 Synthesis of [4-(4′-chloro-5′-phenyloxazol-2′-yl)phenyl]methyl methacrylate derivatives

The [4-(4′-chloro-5′-phenyloxazol-2′-yl)phenyl]methyl methacrylate derivatives were prepared by a three-steps reaction (**Scheme 4.4**). The synthetic route first started from the preparation of 4-(4′-chloro-5′-phenyloxazol-2′-yl)benzaldehyde derivatives by using modification of Fischer synthesis, which is the most efficient method due to the high yield and lack of by-products. Then, the aldehyde group was reduced to alcohol by using sodium borohydride. Finally, this alcohol was reacted with methyl methacryloyl chloride to give a desired monomer. In order to study the effect of substituent group either electron donating or electron withdrawing group was introduced at the para position of the benzene ring.

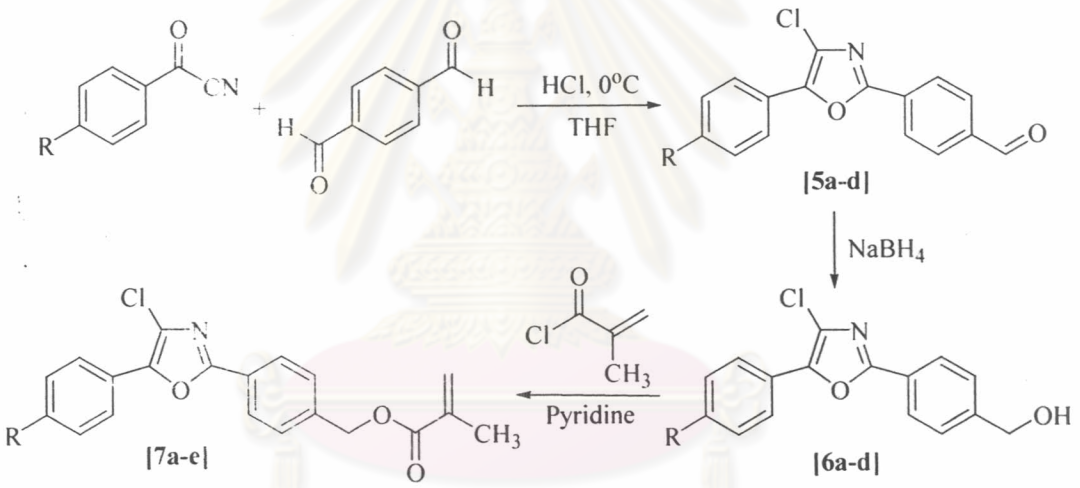


**Scheme 4.4:** Synthetic pathway of [4-(4′-chloro-5′-phenyloxazol-2′-yl)phenyl]methyl methacrylate derivatives

### 4.3.1. Preparation of 4-[4′-chloro-5′-(4-substituted phenyl)oxazol-2′-yl] benzaldehyde [5a-d]

4-(4′-Chloro-5′-phenyloxazol-2′-yl)benzaldehyde derivatives have been obtained from the cyclization reaction of benzoyl cyanide derivative reacting with terephthaldehyde and saturated with hydrogen chloride in one-step reaction. The reaction yield is ranging from 50-75% as summarized in **Table 4.2**. The result is obviously indicative that the electron-withdrawing group, $NO_2$, enhances the reaction

yield comparing with other substituent. While the electron donating, $OCH_3$, retards the reaction yield. The possible mechanism of this cyclization reaction is shown in **Scheme 4.11**.

**Table 4.2:** Percentage yield of 4-(4′-chloro-5′-phenyloxazol-2′-yl)benzaldehyde derivatives

| Compound | Substituent | % Yield |
|---|---|---|
| [5a] | H | 73 |
| [5b] | F | 60 |
| [5c] | $OCH_3$ | 50 |
| [5d] | $NO_2$ | 75 |

**4-(4′-Chloro-5′-phenyloxazol-2′-yl)benzaldehyde [5a]**: From FT-IR spectrum, the absorption peak of cyanide group at 2223 $cm^{-1}$ was disappeared. The absorption bands at 2834, 1699, 1606, 1257 and 1175 $cm^{-1}$ corresponding to CHO stretching, C=O stretching, C=C aromatic stretching and C-Cl stretching, respectively were observed. The absorption band at 1514 $cm^{-1}$ is the characteristic of the –NCO ring. The $^1$H-NMR spectrum of this compound exhibited the characteristic proton of aldehyde at 10.00 ppm. The chemical shifts of the aromatic protons appear at 8.00-8.23 and 7.44-7.56 ppm with correct integration ratios. The peak at $\delta$ = 8.22-8.23 ppm is attributed to proton adjacent to aldehyde group. The down field signal of the C-H resonances associated with the phenyl ring is due to deshielding effect of the aldehyde group. In the $^{13}$C NMR spectrum, the peak at 171.0 $\delta$ is due to carbonyl carbon of aldehyde, the peak at 150.6, 136.5 and 125.4 ppm are characteristic oxazole peaks and the peak around the region 115.5-130.2 ppm is attributed to carbon of aromatic phenyl ring. It is noteworthy that the nitrile signal at 112.3 ppm disappeared. The mass spectrum of 4-(4′-chloro-5′-phenyl-oxazol-2′-yl)-benzaldehyde contained m/z peak of 284 corresponding to the calculated molecular weight and characteristic relative abundance peak of chlorine at M+2 peak of 286 approximately one-third the intensity of the molecular ion peak because of the presence of a molecular ion containing the $^{37}$Cl isotope. **Scheme 4.5** showed the fragmentation pathways. The majority of oxazoles follow the main ring-cleavage fragmentation pattern of unsubstituted oxazole, radical formation, and cleavage of the C-O bond and loss of CO followed by

loss of HCN or nitrile. This compound has also been proved by elemental analysis. The percent found amount of C, H and N was matched to the percent-calculated elemental composition. According to these data, it could be concluded that the product was 4-(4′-chloro-5′-phenyloxazol-2′-yl)benzaldehyde.

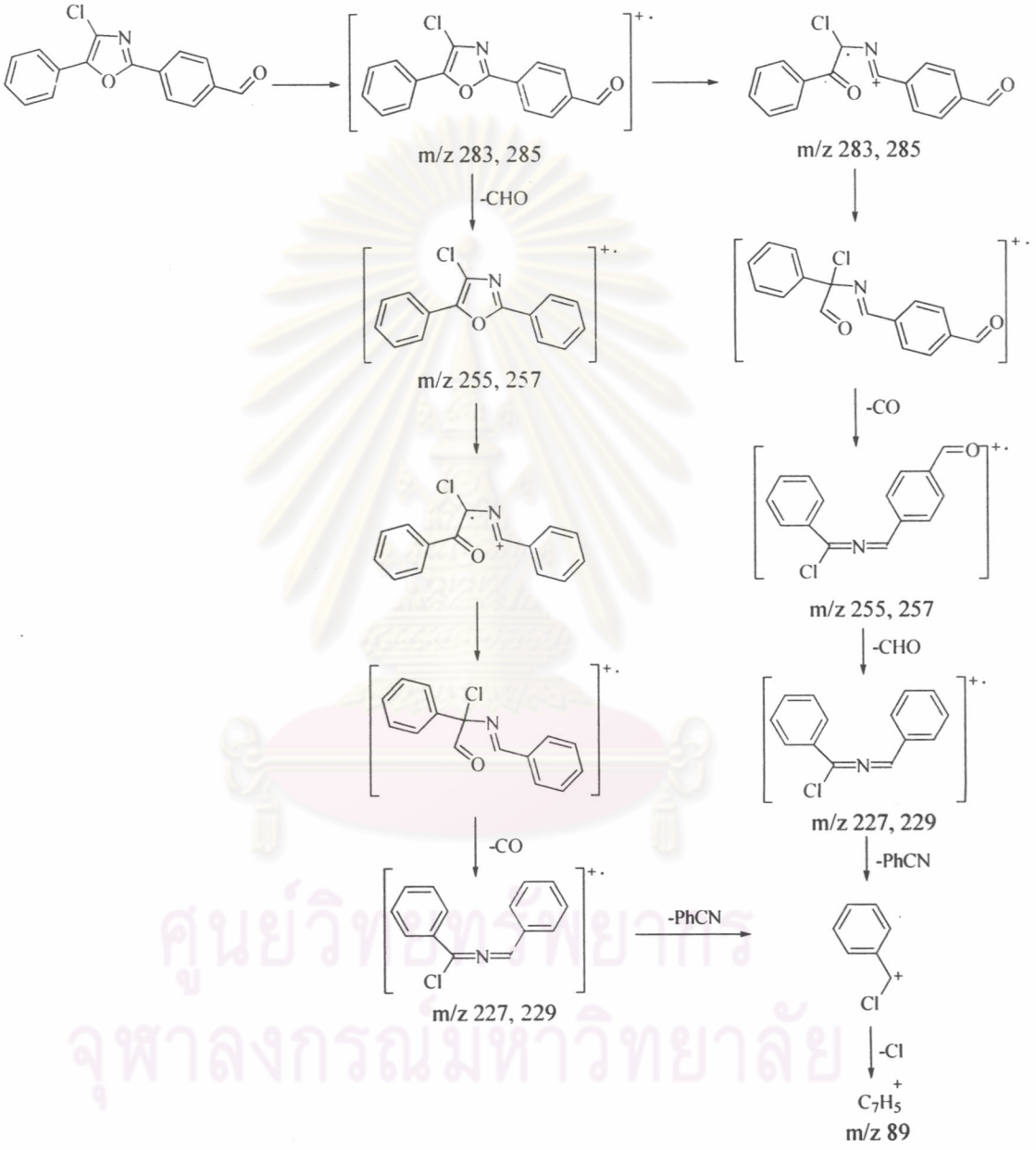


**Scheme 4.5:** Fragmentation pathways of 4-(4′-chloro-5′-phenyloxazol-2′-yl)benzaldehyde

**4-[4′-Chloro-5′-(4-fluorophenyl)oxazol-2′-yl]benzaldehyde [5b]**: The spectrum of this compound reveals several characteristic bands in addition to those seen for 4-(4′-chloro-5′-phenyloxazol-2′-yl)benzaldehyde, as noted above. From FT-IR, the carbonyl stretch is centered at 1699 $cm^{-1}$, which is slightly lower than 4-(4′-chloro-5′-phenyloxazol-2′-yl)benzaldehyde 1704 $cm^{-1}$ due to inductive effect of the fluorine group. The 1237 $cm^{-1}$ band has been assigned to C-F stretch. In the $^{1}H$ NMR spectrum, the chemical shifts of the aromatic protons appear at 7.98-8.28 and 7.22-7.26 ppm with correct integration ratios. In the $^{13}C$ NMR spectrum, it is noteworthy that the signal at 171.1 ppm indicates carbon on aromatic phenyl ring next to fluorine atom. The mass spectrum of 4-[4′-chloro-5′-(4-fluorophenyl)oxazol-2′-yl] benzaldehyde contained m/z peak of 301 corresponding to the calculated molecular weight and characteristic relative abundance peak of chlorine at M+2 peak of 303 approximately one-third the intensity of the molecular ion peak because of the presence of a molecular ion containing the $^{37}Cl$ isotope. This compound has also been proved by elemental analysis. The percent found amount of C, H and N was matched with the percent-calculated elemental composition. According to these data, it could be concluded that the product was 4-[4′-chloro-5′-(4-fluorophenyl)oxazol-2′-yl]-benzaldehyde.

**4-[4′-Chloro-5′-(4-methoxyphenyl)oxazol-2′-yl]benzaldehyde [5c]**: The spectrum of this compound reveals several characteristic bands in addition to those seen for 4-(4′-chloro-5′-phenyloxazol-2′-yl)benzaldehyde, as noted above. From FT-IR, the 1257 $cm^{-1}$ band has been assigned to C-O-C stretch. In the $^{1}H$ NMR spectrum, the chemical shifts of the aromatic protons appear at 7.92-8.26 and 7.05-7.07 ppm with correct integration ratios. The up field signals of the C-H resonances associated with the phenyl ring between $\delta$ = 7.05-7.07 ppm are due to shielding effect of the methoxy group. In the $^{13}C$ NMR spectrum, it is should be noted that the signal at 55.4 ppm indicates carbon of methoxy group. The mass spectrum of 4-[4′-chloro-5′-(4-methoxyphenyl)oxazol-2′-yl]benzaldehyde contained m/z peak of 313 corresponding to the calculated molecular weight and characteristic relative abundance peak of chlorine at M+2 peak of 315 approximately one-third the intensity of the molecular ion peak because of the presence of a molecular ion containing the $^{37}Cl$ isotope. Elemental CHN analyses indicated the presence of a methoxy functionality. According to these

data, it could be concluded that the product was 4-[4′-chloro-5′-(4-methoxyphenyl)-oxazol-2′-yl]benzaldehyde.

**4-[4′-Chloro-5′-(4-nitrophenyl)oxazol-2′-yl]benzaldehyde [5d]**: The spectrum of this compound reveals several characteristic bands in addition to those seen for 4-(4′-chloro-5′-phenyloxazol-2′-yl)benzaldehyde, as noted above. From FT-IR, the 1339 $cm^{-1}$ band has been assigned to C-N stretch. In the $^{1}H$ NMR spectrum, the chemical shifts of the aromatic protons appear at 8.31-8.42 and 8.09-8.20 ppm with correct integration ratios. The down field signals of the C-H resonances associated with the phenyl ring is due to deshielding effect of the nitro group. In the $^{13}C$ NMR spectrum, it should be noted that the field signal at 148.4 ppm indicates the nitro substituent at the para position of phenyl moiety. Since nitro is a strong electron-withdrawing group, it causes a downfield shift of aromatic protons. The mass spectrum of 4-[4′-chloro-5′-(4-nitrtophenyl)oxazol-2′-yl]benzaldehyde contained m/z peak of 328 corresponding to the calculated molecular weight and characteristic relative abundance peak of chlorine at M+2 peak of 330 approximately one-third the intensity of the molecular ion peak because of the presence of a molecular ion containing the $^{37}Cl$ isotope. Elemental CHN analyses indicated the presence of a nitro functionality. According to these data, it could be concluded that the product was 4-[4′-chloro-5′-(4-nitrophenyl)oxazol-2′-yl]benzaldehyde.

### 4.3.2. Preparation of [4-(4′-chloro-5′-phenyloxazol-2′-yl)-phenyl]methanol derivatives

[4-(4′-Chloro-5′-phenyl-oxazol-2′-yl)-phenyl]methanol derivatives have been obtained from the reduction of aldehyde to alcohol using sodium borohydride in tetrahydrofuran at room temperature. In a reduction by sodium borohydride, hydride ion adds to the partially positive carbonyl carbon, which leaves a negative charge on the carbonyl oxygen. Reaction of this intermediate with aqueous acid gives the alcohol.

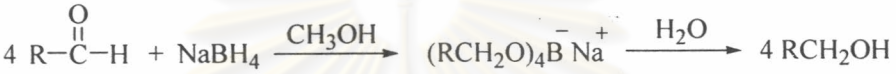

**Scheme 4.6:** Reduction of aldehyde to alcohol

The reaction gave quite a high yield in the range of 75-85% without the need to isolate as shown in **Table 4.3**. Either the electron donating or electron withdrawing group at the para position of phenyl moiety exhibited a reaction yield in the same range because the position of substituent group is far from the carboyl group and does not play an important role.

**Table 4.3:** Percentage yield of [4-(4′-chloro-5′-phenyloxazol-2′-yl)phenyl]methanol derivatives

| Compound | Substituent | % Yield |
|---|---|---|
| [6a] | H | 85 |
| [6b] | F | 80 |
| [6c] | $OCH_3$ | 85 |
| [6d] | $NO_2$ | 75 |

**[4-(4′-Chloro-5′-phenyloxazol-2′-yl)phenyl]methanol [6a]**: From FT-IR spectrum, the absorption peak of carbonyl group of aldehyde at 1704 $cm^{-1}$ was absent. The broad absorption peak of O-H stretching at 3300 $cm^{-1}$ and C-O stretching at 1200 $cm^{-1}$ were found. The $^1$H-NMR spectrum of [4-(4′-chloro-5′-phenyl-oxazol-2′-yl)phenyl]methanol are somewhat different form that of the 4-(4′-chloro-5′-phenyl-oxazol-2′-yl)benzaldehyde, a starting material. Notable differences are the

characteristic singlet methylene photon adjacent to benzene ring at 4.84 ppm and a broad singlet peak of hydroxyl photon at 1.96 ppm. The chemical shift of aldehyde photon at approximately 10 ppm was disappeared. In the $^{13}C$ NMR spectrum, the peak at 171.0 δ due to carbonyl carbon of aldehyde was disappeared. The peak at 150.6, 136.5 and 125.4 ppm are characteristic oxazole peaks. It is noteworthy that the peak at 68.5 ppm is attributed to methylene carbon of aromatic phenyl ring. The mass spectrum of 4-(4′-chloro-5′-phenyloxazol-2′-yl)phenyl]methanol derivatives contained m/z peak of 286 corresponding to the calculated molecular weight and characteristic relative abundance peak of chlorine at M+2 peak of 288 approximately one-third the intensity of the molecular ion peak. The characteristic pattern of the peak was presented that it had a chlorine atom due to the M+2 peak. **Scheme 4.7** showed the fragmentation pathway, which exhibited benzylic cleavage product from the initial radical cation. This compound has also been proved by elemental analysis. The percent found amount of C, H and N was matched to the percent-calculated elemental composition. According to these data, it could be concluded that the product was [4-(4′-chloro-5′-phenyloxazol-2′-yl)phenyl]methanol.

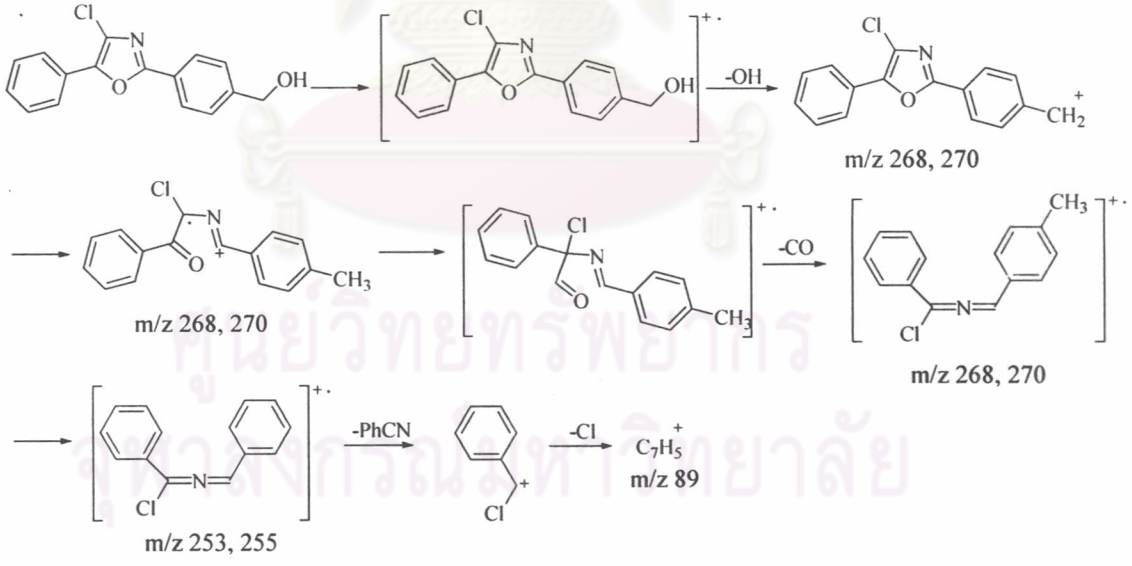


**Scheme 4.7:** Fragmentation pathway of 4-(4′-chloro-5′-phenyloxazol-2′-yl)phenyl]methanol

**{4-[4′-Chloro-5′-(4-fluorophenyl)oxazol-2′-yl]phenyl}methanol [6b]:** The spectrum of this compound reveals several characteristic bands in addition to those seen for 4-(4′-chloro-5′-phenyloxazol-2′-yl)phenyl]methanol, as noted above. From FT-IR, the 1237 $cm^{-1}$ band has been assigned to C-F stretch. In the $^{1}H$ NMR spectrum, the chemical shifts of the aromatic protons appear at 7.95-8.10 and 7.19-7.53 ppm with correct integration ratios. The upfield signals of the C-H resonances associated with the phenyl ring between $\delta$ = 7.19-7.23 ppm comparing to unsubstituent are due to shielding effect of the fluorine group substituent. In the $^{13}C$ NMR spectrum, it is noteworthy that the signal at 162.1 ppm indicates carbon on aromatic phenyl ring next to fluorine atom. The mass spectrum of {4-[4′-chloro-5′-(4-fluorophenyl)oxazol-2′-yl]-phenyl}methanol contained m/z peak of 303 corresponding to the calculated molecular weight and characteristic relative abundance peak of chlorine at M+2 peak of 305 approximately one-third the intensity of the molecular ion peak because of the presence of a molecular ion containing the $^{37}Cl$ isotope. This compound has also been proved by elemental analysis. The percent found amount of C, H and N was matched to the percent-calculated elemental composition. According to these data, it could be concluded that the product was {4-[4′-chloro-5′-(4-fluorophenyl)oxazol-2′-yl]phenyl} methanol.

**{4-[4′-Chloro-5′-(4-methoxyphenyl)oxazol-2′-yl]phenyl}methanol [6c]:** The spectrum of this compound reveals several characteristic bands in addition to those seen for 4-(4′-chloro-5′-phenyloxazol-2′-yl)phenyl]methanol, as noted above. From FT-IR, the 1252 $cm^{-1}$ band has been assigned to C-O-C stretch. In the $^{1}H$ NMR spectrum, the chemical shifts of the aromatic protons appear at 7.91-8.10 and 7.04-7.53 ppm with correct integration ratios. The up field signals of the C-H resonances associated with the phenyl ring between $\delta$ = 7.04-7.06 ppm are due to shielding effect of the methoxy group by resonance effect. The peak at 3.91 $\delta$ also indicates methyl protons due to a methoxy group. In the $^{13}C$ NMR spectrum, the signal at 56.0 ppm indicates methyl carbon of methoxy group is formed. The mass spectrum of {4-[4′-chloro-5′-(4-methoxyphenyl)oxazol-2′-yl]phenyl}methanol contained m/z peak of 315 corresponding to the calculated molecular weight and characteristic relative abundance peak of chlorine at M+2 peak of 317 approximately one-third the intensity of the molecular ion peak because of the presence of a molecular ion containing the $^{37}Cl$ isotope. This

compound has also been proved by elemental analysis. Elemental CHN analyses indicated the presence of a methoxy functionality. According to these data, it could be concluded that the product was {4-[4′-chloro-5′-(4-methoxyphenyl)-oxazol-2′-yl]phenyl} methanol.

**{4-[4′-Chloro-5′-(4-nitrophenyl)oxazol-2′-yl]phenyl}methanol [6d]:** The spectrum of this compound reveals several characteristic bands in addition to those seen for 4-(4′-chloro-5′-phenyloxazol-2′-yl)phenyl]methanol, as noted above. From FT-IR, the 1334 $cm^{-1}$ band has been assigned to C-N stretch. In the $^{1}H$ NMR spectrum, the chemical shifts of the aromatic protons appear at 8.12-8.39 and 7.55-7.57 ppm with correct integration ratios. The down field signals of the C-H resonances associated with the phenyl ring is due to shielding effect of the nitro group by resonance effect. In the $^{13}C$ NMR spectrum, it is noteworthy that the signal at 148.4 ppm due to a carbon on the aromatic phenyl ring next to fluorine atom is formed. The mass spectrum of {4-[4′-chloro-5′-(4-nitrophenyl)oxazol-2′-yl]phenyl}methanol contained m/z peak of 330 corresponding to the calculated molecular weight and characteristic relative abundance peak of chlorine at M+2 peak of 332 approximately one-third the intensity of the molecular ion peak because of the presence of a molecular ion containing the $^{37}Cl$ isotope. This compound has also been proved by elemental analysis. Elemental CHN analyses indicated the presence of a nitro functionality. According to these data, it could be concluded that the product was {4-[4′-chloro-5′-(4-nitrophenyl)oxazol-2′-yl]-phenyl}methanol.

### 4.3.3. Preparation of [4-(4′-chloro-5′-phenyloxazol-2′-yl)phenyl]methyl methacrylate derivatives

[4-(4′-Chloro-5′-phenyloxazol-2′-yl)phenyl]methyl methacrylate derivatives have been obtained from the nucleophilic substitution reaction between 4-(4′-chloro-5′-phenyloxazol-2′-yl)phenyl]methanol derivatives and methyl methacryloyl chloride using pyridine as a base.

Both the carbonyl oxygen and the chloride atom withdraw electron density from the acyl carbon atom, making it strongly electrophilic. Hydroxy ion is a good nucleophile (donor of an electron pair) because the oxygen has unshared pairs of electrons and a negative charge. Acid chlorides react with alcohols to give esters through a nucleophilic substitution by the addition-elimination mechanism. Attack by the alcohol at the electrophilic carbonyl group gives a tetrahedral intermediate. Loss of chloride and deprotonation give the ester.

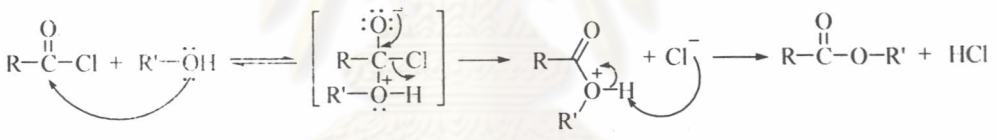

**Scheme 4.8:** Nucleophilic substitution reaction of acid chloride

This reaction gave yields in the range of 50-60% as shown in **Table 4.4**. From the mechanism, the substituent, which increases the electrophilicity of carbonyl, can enhance the nucleophilic substitution reaction. In this case, the substituent can either be an electron donating or an electron withdrawing group at para position of phenyl moiety located quite far from reaction center. Therefore, the yield of both electron donating and electron withdrawing groups are in the same range.

**Table 4.4:** Percentage yield of [4-(4′-chloro-5′-phenyloxazol-2′-yl)phenyl]methyl methacrylate derivatives

| Compound | Substituent | % Yield |
|---|---|---|
| [7a] | H | 50 |
| [7b] | F | 55 |
| [7c] | $OCH_3$ | 60 |
| [7d] | $NO_2$ | 50 |

**[4-(4′-Chloro-5′-phenyloxazol-2′-yl)phenyl]methyl methacrylate [7a]:** From FT-IR spectrum, the absorption peak of O-H stretching at 3300 $cm^{-1}$ was absent and a strong absorption peak of and C=O stretching from acrylate moiety at 1700 $cm^{-1}$ were found. The structure of the monomer was confirmed by NMR spectroscopy. The $^1H$ NMR spectrum in **Figure 4.2** shows the characteristic 2 singlet signals from $=CH_2$ at 6.23 and 5.67 ppm ("e" in spectrum) and a singlet signal of methylene photon adjacent to the ring at 5.29 ppm ("f" in spectrum).

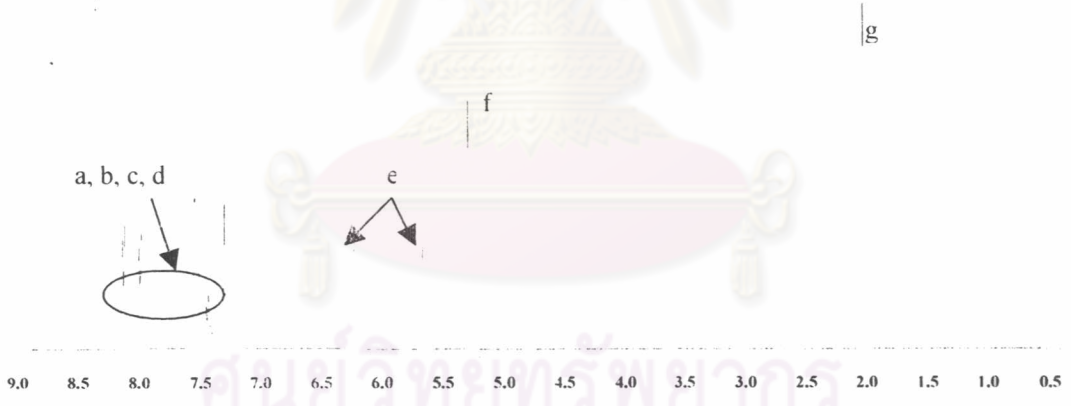


**Figure 4.2:** $^1H$ NMR spectrum of [4-(4′-chloro-5′-phenyloxazol-2′-yl)phenyl]methyl methacrylate

The $^{13}C$ NMR spectrum revealed the presence of vinyl group at 121.4 ppm and the peak at 18.4 ppm indicated methyl carbon adjacent to vinyl group. The mass spectrum of [4-(4′-chloro-5′-phenyloxazol-2′-yl)phenyl]methyl methacrylate derivatives contained m/z peaks corresponding to the calculated molecular weight and characteristic relative abundance peak of chlorine at M+2 peak approximately one-third the intensity of the molecular ion peak. The characteristic pattern of the peak was presented that it had a chlorine atom due to the M+2 peak. **Scheme 4.9** showed

the fragmentation pathway, which exhibited benzylic cleavage product from the initial radical cation. The elemental analysis of [4-(4′-chloro-5′-phenyloxazol-2′-yl)phenyl]methyl methacrylate derivatives was preformed. The result showed that the percent found amount of C, H and N was corresponding to the percent-calculated elemental composition.

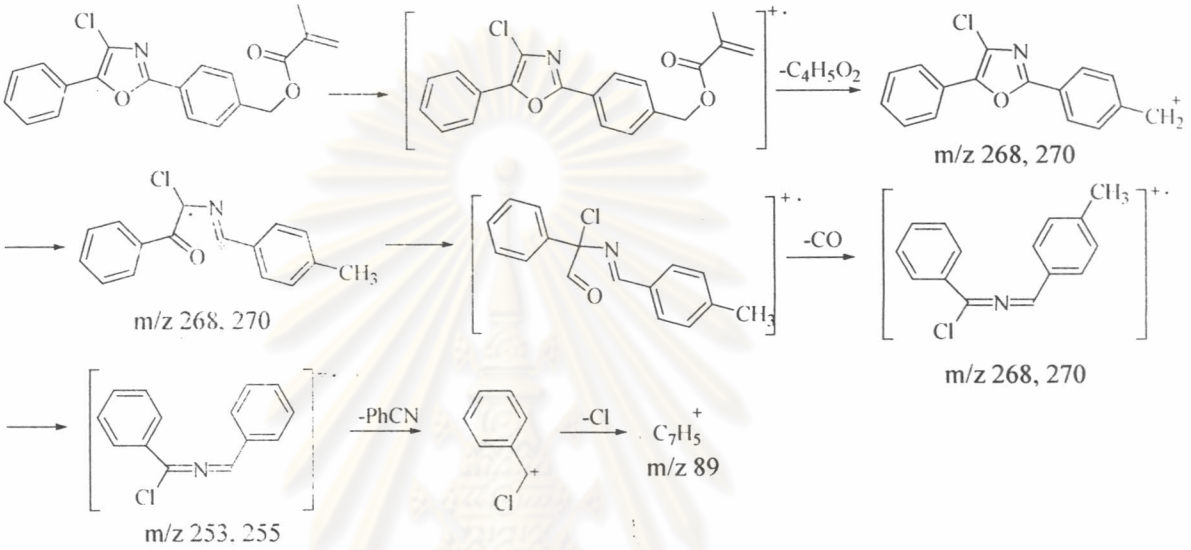


**Scheme 4.9:** Fragmentation pathway of [4-(4′-chloro-5′-phenyloxazol-2′-yl)phenyl] methyl methacrylate

**{4-[4′-Chloro-5′-(4-fluorophenyl)oxazol-2′-yl]phenyl}methyl methacrylate [7b]:** The spectrum of this compound show a set of peak, which are virtually the same as to those seen for [4-(4′-chloro-5′-phenyloxazol-2′-yl)phenyl]methyl methacrylate, as noted above. From FT-IR, the 1293 $cm^{-1}$ band has been assigned to C-F stretch. In the $^{1}H$ NMR spectrum, the chemical shifts of the aromatic protons appear at 7.94-8.11 and 7.20-7.53 ppm with correct integration ratios. The upfield signals of the C-H resonances associated with the phenyl ring between $\delta$ = 7.10-7.24 ppm comparing to unsubstituent are due to shielding effect of the fluorine group substituent. In the $^{13}C$ NMR spectrum, it is noteworthy that the signal at 162.1 ppm indicates carbon on aromatic phenyl ring next to fluorine atom. The mass spectrum of {4-[4′-chloro-5′-(4-fluorophenyl)oxazol-2′-yl]phenyl}methyl methacrylate contained m/z peak of 372 corresponding to the calculated molecular weight and characteristic relative

abundance peak of chlorine at M+2 peak of 374 approximately one-third the intensity of the molecular ion peak because of the presence of a molecular ion containing the $^{37}Cl$ isotope. This compound has also been proved by elemental analysis. The percent found amount of C, H and N was matched to the percent-calculated elemental composition. According to these data, it could be concluded that the product was {4-[4′-chloro-5′-(4-fluorophenyl)oxazol-2′-yl]phenyl}methyl methacrylate.

**{4-[4′-Chloro-5′-(4-methoxyphenyl)oxazol-2′-yl]phenyl}methyl methacrylate [7c]**: The spectrum of this compound show a set of peak, which are virtually the same as to those seen for [4-(4′-chloro-5′-phenyloxazol-2′-yl)phenyl]methyl methacrylate, as noted above. In the $^{1}H$ NMR spectrum, the chemical shifts of the aromatic protons appear at 7.90-8.10 and 7.04-7.53 ppm with correct integration ratios. The upfield signals of the C-H resonances associated with the phenyl ring between $\delta$ = 7.04-7.06 ppm comparing to unsubstituent are due to shielding effect of the methoxy group substituent. In the $^{13}C$ NMR spectrum, the signal at 56.2 ppm due to methoxy carbon on aromatic phenyl ring is formed. The mass spectrum of {4-[4′-chloro-5′-(4-methoxyphenyl)oxazol-2′-yl]phenyl}methyl methacrylate contained m/z peak of 383 corresponding to the calculated molecular weight and characteristic relative abundance peak of chlorine at M+2 peak of 385 approximately one-third the intensity of the molecular ion peak because of the presence of a molecular ion containing the $^{37}Cl$ isotope. This compound has also been proved by elemental analysis. Elemental CHN analyses indicated the presence of a methoxy functionality. According to these data, it could be concluded that the product was {4-[4′-chloro-5′-(4-methoxyphenyl)oxazol-2′-yl]phenyl}methyl methacrylate.

**{4-[4′-Chloro-5′-(4-nitrophenyl)oxazol-2′-yl]phenyl}methyl methacrylate [7d]:** The spectrum of this compound show a set of peak, which are virtually the same as to those seen for [4-(4′-chloro-5′-phenyloxazol-2′-yl)phenyl]methyl methacrylate, as noted above. From FT-IR, the 1334 $cm^{-1}$ band has been assigned to C-N stretch. The peak around the region of 1500-1700 $cm^{-1}$ is due to the C=O stretch and N=O stretch. In the $^{1}H$ NMR spectrum, the chemical shifts of the aromatic protons appear at 8.13-8.40 and 7.53-7.57 ppm with correct integration ratios. The down field signals of the C-H resonances associated with the phenyl ring are due to electron-withdrawing effect of

the nitro group substituent. In the $^{13}C$ NMR spectrum, the signal at 148.4 ppm due to carbon on aromatic phenyl ring adjacent to nitro group is formed. The mass spectrum of {4-[4′-chloro-5′-(4-nitrophenyl)oxazol-2′-yl]phenyl}methyl methacrylate contained m/z peak of 398 corresponding to the calculated molecular weight and characteristic relative abundance peak of chlorine at M+2 peak of 400 approximately one-third the intensity of the molecular ion peak because of the presence of a molecular ion containing the $^{37}Cl$ isotope. This compound has also been proved by elemental analysis. Elemental CHN analyses indicated the presence of a nitro functionality. According to these data, it could be concluded that the product was {4-[4′-chloro-5′-(4-nitrophenyl)oxazol-2′-yl]phenyl}methyl methacrylate.

## 4.4 Hydrogenation of Nntro compound

The most frequently used nitro-group hydrogenation catalysts are palladium or platinum on carbon and Raney nickel. Hydrogenations of aromatic nitro compounds have been frequently studied, and the reaction pathway is well-known (**Scheme 4.10**). In these reactions, the nitroso compound and the hydroxylamine have been observed as intermediates. while a series of side reactions might lead to the formation of hydrazo compounds, which can sometimes also be isolated. In general, the activity and selectivity of this reaction depends on the catalysts as well as on the reaction conditions. Alcohols, ethyl acetate, aromatics and aqueous acid solutions are often used as reaction solvents; many processes are performed commercially without solvent. For partial hydrogenation, additives are often employed to improve selectivity. Reactions are typically carried out between 5 and 150°C with 1 to 25 atmospheres $H_2$ pressure. Exact conditions depend on the desired final product.

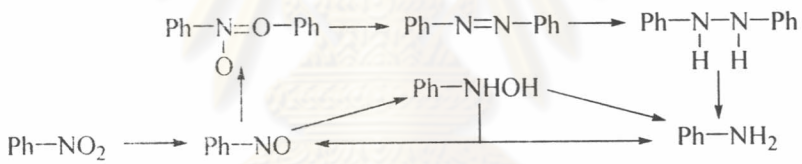


**Scheme 4.10:** Hydrogenation of an aromatic nitro compound

**{4-[4′-Chloro-5′-(4-aminophenyl)oxazol-2′-yi]phenyl}methyl methacrylate [7e]** was synthesized by hydrogenation of {4-[4′-chloro-5′-(4-nitrophenyl)oxazol-2′-yl]phenyl}methyl methacrylate using 5% Pd/C. The reaction yield is only 40% because C=C bond in the starting material can be reduced as well. This by-product was detected by TLC. When the reaction time is longer than 10 mins, the number of by-product was increased. The reaction was extensively characterised to confirm the formation of $NH_2$. The strong IR bands for the nitro group at 1350 and 1550 $cm^{-1}$ completely disappear after the reaction with the appearance of bands at 3355-3439 $cm^{-1}$ related to the amine. Elemental CHN analyses indicated the presence of a $NH_2$ functionality. Detailed $^{1}H$ and $^{13}C$ characterisation of the reaction product clearly show completely different chemical shifts of the amino product compared to the starting material.

## 4.5 Effect of the aromatic substituents on cyclization reaction

As a result, several 4-chloro-2,5-diphenyloxazoles were readily obtained as single products with high yield. A plausible mechanism of this reaction is proposed based on an experimental results and observation.

Several 4-chloro-2,5-diphenyloxazole derivatives were prepared by a one step reaction. The interaction of benzoyl cyanide derivatives with the corresponding benzaldehyde always leads to the desired oxazole product via the corresponding acylimidoyl chloride (**Scheme 4.11**). The initial addition of HCl onto the cyano group gave acylimidoyl chloride. Then, acylimidoyl chloride promptly attacked the aldehyde carbonyl carbon. Subsequently, ring closure is feasible, especially in the presence of an additional electron withdrawing $R_1$ substituents.

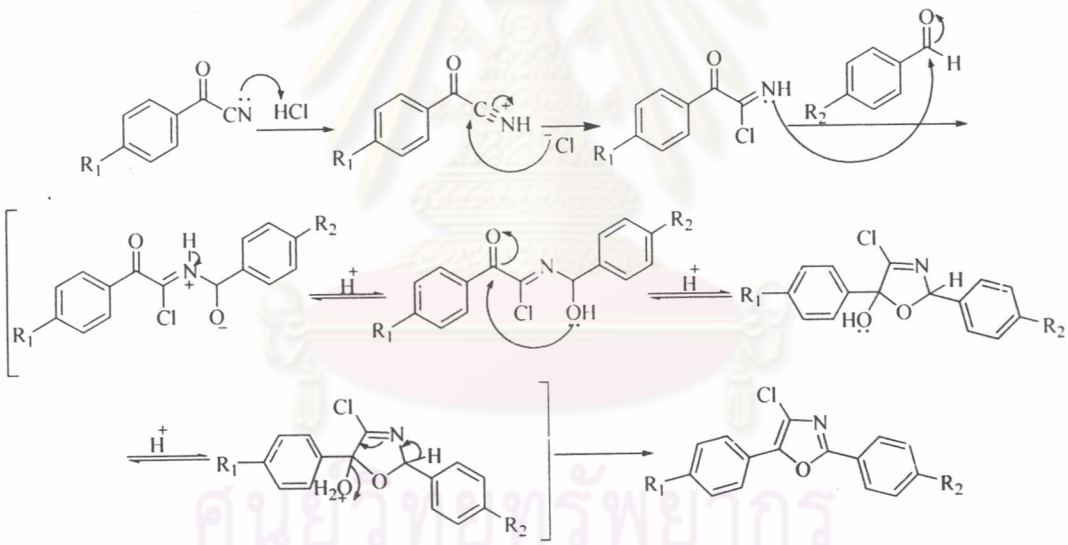

**Scheme 4.11:** Mechanism of oxazole formation

From the experimental results, $NO_2$ substituent of $R_1$ **[5d]**, gave the highest yield (75%) follow with H **[5a]**, F **[5b]** and OMe **[5c]**, respectively, when $R_2$ group is the same. This strong withdrawing group presumably facilitates the ring formation by increasing the electrophilicity of carbonyl intermediate through the resonance effect. On the other hand, introduction of electron-donating groups (OMe) result a low yield because these groups possibly decrease the nucleophilicity of the nitrogen atom of the benzoyl cyanide and cause some side reactions resulting in a reduction of oxazole formation. Therefore, 4-[4-chloro-5-(4-methoxyphenyl-oxazol-2-yl]benzaldehyde,

formation. Therefore, 4-[4′-chloro-5′-(4-methoxyphenyl-oxazol-2′-yl]benzaldehyde, **[5c]**, gave a lowest yield comparing with the other. It is noteworthy that the F substituent can serve as an electron-withdrawing group from a carbon atom through the sigma bond but the reaction yield is lower comparing with $NO_2$. This case indicated that the resonance effect might play a dominant role.

It can be seen from the experimental results that the yields are favorable with those benzaldehyde bearing electron-withdrawing substituents $R_2$ on its benzene rings. Introduction of CHO group **[5a]** at $R_2$ resulted in increase of yields comparing with Et group **[2]**.

Additionally, this cyclization reaction required a strong nucleophile thus, the water is eliminated by freshly dry tetrahydrofuran and dry sodium chloride overnight at 100°C in the oven before use. Otherwise, a hydroxyl anion from water can acted as another nucleophile and terminated the cyclization reaction.

## 4.6 Free-radical polymerization

### 4.6.1 Characterization

Acrylate monomers, [4-(4′-chloro-5′-phenyloxazol-2′-yl)phenyl]methyl methacrylate derivatives, were copolymerized with MMA under radical condition in dry THF at 60°C for 48 h. After product purification, the polymerization was monitored by FT-IR spectroscopy, by checking the disappearance in the spectra of the absorption at approximately 1600 $cm^{-1}$("a"), related to the methacrylic double bond, and the contemporary appearance of the band at 1724-1730 $cm^{-1}$("b" from Figure 4.3), related to the carbonyl stretching vibration of the $\alpha$, $\beta$ saturated methacrylic ester group, shift to higher frequency by *ca.* 10 $cm^{-1}$ with respect to the corresponding band of the monomer (**Figure 4.4**). Accordingly, in the $^1$H-NMR spectra of polymeric derivatives the resonance of the vinylidenic proton of monomeric methylacrylate disappeared. All substituents gave almost the same aromatic proton chemical shifts in the range of 7.30-8.20 ppm as shown in **Figure 4.5**.

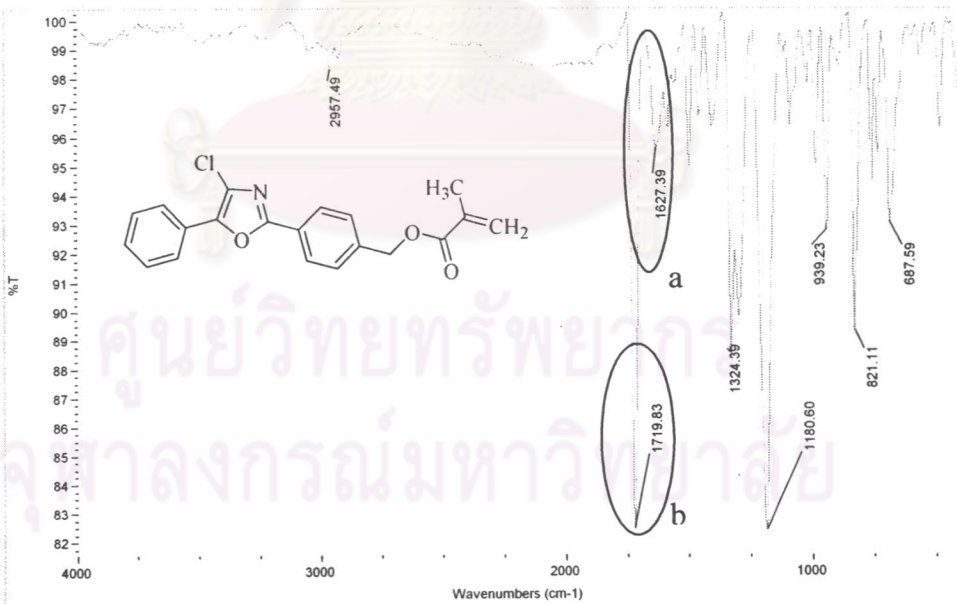


**Figure 4.3:** FT-IR spectrum of acrylate monomer **[7a]**

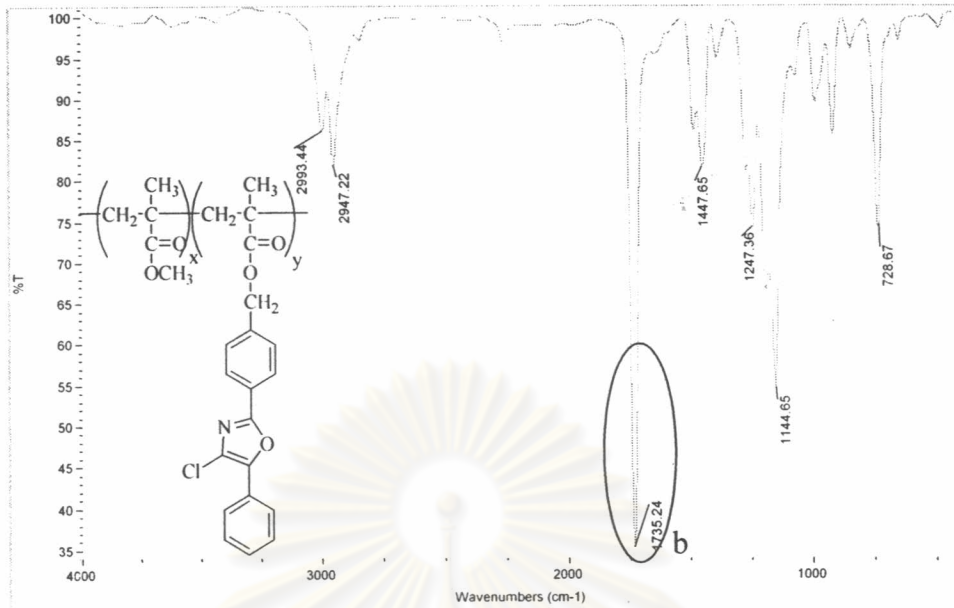


**Figure 4.4:** FT-IR spectrum 5% ratio of free radical polymer **[P5]**


**Figure 4.5:** $^{1}$H-NMR spectra of acrylate monomer **[7a]** and 5% ratio of free radical polymer **[P5]**

For all the polymers, $^{1}$H NMR and FT-IR show no evidence of unreacted vinyl group, indicating that separation of the monomer reactants from the polymer product was essentially complete.

The molar composition of copolymers can be calculated by $^1$H-NMR spectroscopy comparing the integration of the singlet signal due to the methyl ester group of MMA, located at 3.63 ppm ("a" from Figure 4.5), and the methylene proton of [4-(4-chloro-5-phenyloxazol-2-yl)phenyl]methyl methacrylate derivatives at 5.30 ppm ("b" from Figure 4.5), after subtraction of the contribution given to the integral by the overlapped resonance methylene photons in α position to phenyl of [4-(4-chloro-5-phenyloxazol-2-yl)phenyl]methyl methacrylate.

**Table 4.5:** Feed ratio for preparation of polymers

| Polymer | Substituents (R) | Feed Ratio (Mole %) | Average %Composition of scintillant | |
|---|---|---|---|---|
| | | scintillant/MMA | Theoretical | Calculation |
| [P1] | R = H | 1/99 | 1 | 0.27 |
| [P5] | | 5/95 | 5 | 1.61 |
| [Pf1] | R = F | 1/99 | 1 | 0.41 |
| [Pf5] | | 5/95 | 5 | 1.80 |
| [Pm1] | R = $OCH_3$ | 1/99 | 1 | 0.19 |
| [Pm5] | | 5/95 | 5 | 1.14 |
| [Pn1] | R= $NO_2$ | 1/99 | 1 | 0.42 |
| [Pn5] | | 5/95 | 5 | 1.33 |
| [Pnh2] | R= $NH_2$ | 5/95 | 5 | 1.27 |

From **Table 4.5**, it can be clearly seen that increased in percent feed of fluorescent monomers leads to a slightly increase in exactly percent composition of this monomer in the copolymer. It was proposed that the reactivity of the methyl methacrylate radical is higher than the fluorescence monomer due to the steric hindrance of the acrylic oxazole monomer.

### 4.6.2 Determination of molecular weight

The molecular weights and polydispersities of free radical polymers at different ratios were shown in **Table 4.6**.

**Table 4.6:** Polymerization results of different compositions

| Polymer | *Mn* | *Mw* | PDI |
|---|---|---|---|
| [P1] | 16,722 | 22,941 | 1.36 |
| [P5] | 12,157 | 17,128 | 1.41 |
| [Pf1] | 22,494 | 41,545 | 1.84 |
| [Pf5] | 14,284 | 21,562 | 1.51 |
| [Pm1] | 17,266 | 28,778 | 1.66 |
| [Pm5] | 13,909 | 19,763 | 1.42 |
| [Pn1] | 51,015 | 81,624 | 1.60 |
| [Pn5] | 54,799 | 73,978 | 1.35 |
| [Pnh2] | 17,453 | 29,497 | 1.69 |

The molecular weights of these copolymers were determined by GPC using monodisperse polystyrenes as the standard. As depicted in **Table 4.6**, the weight-average molecular weights (*M*w) are between 17,128 and 81,624 with polydispersity indices (*M*w/*M*n) in the range 1.35-1.69. It should be noted that polymer **[Pn1]** and **[Pn5]**, which are contain nitro groups at the para position of 4-chloro-2,5-diphenyloxazole moiety, exhibited a higher molecular weight than others.

### 4.6.3 Determination of thermal properties

The thermal stability of all polymeric derivatives, as determined by TGA, was relatively high. Most of copolymers were not as thermally stable as PMMA (260°C). The temperatures at which they underwent 5% weight losses (*Td*) when subjected to TGA under $N_2$ with a heating rate of 10°C/min ranged from 247-280°C, indicative of a remarkable presence of strong dipolar interactions in the solid state between the chromophores located in the macromolecular side chains and characterized by a high charge delocalization. Surprisingly, the polymers containing $NO_2$ substituents **[Pn1]** and **[Pn5]** were more thermally stable than PMMA with *Td* of 280°C. A plausible explanation is the strongest polar of nitro groups. The bulky 4-chloro-2,5-diphenyloxazole moieties also serve to increase the free volume of the polymers. Therefore, *Td* of these free radical polymers is lower than PMMA.

**Table 4.7:** Thermal properties of free radical polymers

| Polymer | *Tg* (°C) | *Td* (°C) |
|---|---|---|
| [P1] | 120 | 247 |
| [P5] | 114 | 247 |
| [Pf1] | 124 | 252 |
| [Pf5] | 121 | 252 |
| [Pm1] | 129 | 254 |
| [Pm5] | 118 | 254 |
| [Pn1] | 125 | 280 |
| [Pn5] | 128 | 280 |
| [Pnh2] | 125 | 265 |

Only second order transitions originated by glass transitions were observed in the material by DSC measurements, thus suggesting that the macromolecules are substantially amorphous in the solid state. The decrease of crystallinity is caused by addition of 4-chloro-2,5-diphenyloxazole in the pendent chain.

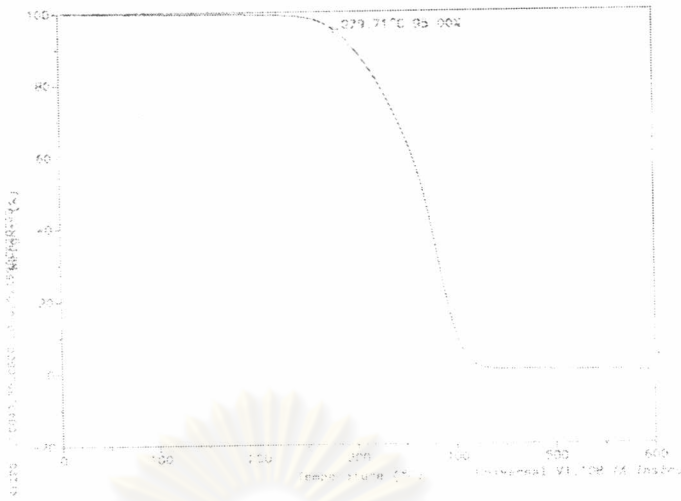

**Figure 4.6:** Typical thermogravimetric curve of free radical polymer in $N_2$

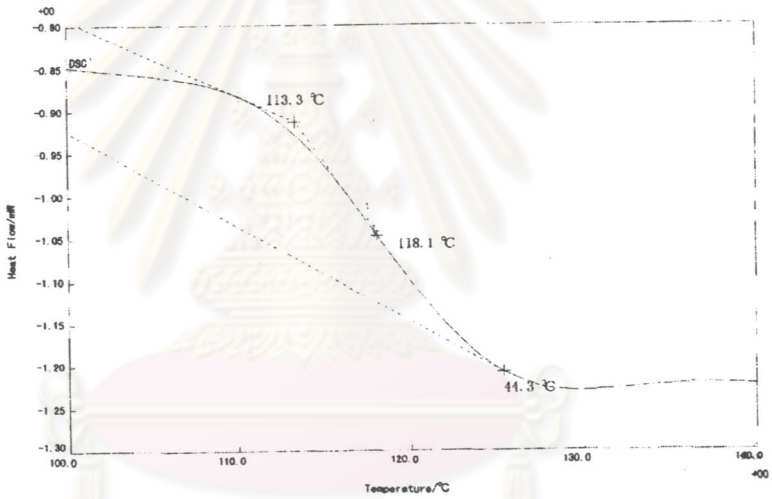


**Figure 4.7:** Typical DSC thermogram of free radical polymer

### 4.6.4 Polymer solubility

The free radical polymers containing 4-chloro-2,5-diphenyloxazole derivatives as a pendent chain show good solubility in a number of common organic solvents. **Table 4.8** summarizes the results of qualitative solubility tests.

**Table 4.8:** Solubility of free-radical polymers

| Polymer | THF | Toluene | $CHCl_3$ | NMP | DMPU |
|---|---|---|---|---|---|
| [P1] | + | + | + | + | + |
| [P5] | + | + | + | + | + |
| [Pf1] | + | + | + | + | + |
| [Pf5] | + | + | + | + | + |
| [Pm1] | + | + | + | + | + |
| [Pm5] | + | + | + | + | + |
| [Pn1] | + | + | + | + | + |
| [Pn5] | + | + | + | + | + |
| [Pnh2] | + | + | + | + | + |

(+) Soluble (-) insoluble (±) partially soluble

**Part B: Preparation of condensation polymers**

### 4.7 Preparation of 4-chloro-2,5-bis-(4′-fluorophenyl)oxazole monomer

To obtained di-functionalized monomer containing 4-chloro-2,5-diphenyl oxazole, 4-chloro-2,5-bis-(4′-fluorophenyl)oxazole was prepared in two steps starting from 4-fluorobenzoyl chloride. First, 4-fluorobenzoyl chloride was treated with CuCN in acetonitrile to prepare 4-fluorobenzoyl cyanide (yield 85%). In the next step, the prepared 4-fluorobenzoyl cyanide was reacted with 4-fluorobenzaldehyde to obtain 4-chloro-2,5-bis-(4-fluorophenyl)oxazole monomer. The oxazole moiety on the para position to each fluorine substituent on the same benzene ring should exhibit strong electron-withdrawing effect and are expect to function as an activating group for the nucleophilic substitution of fluorine atom via stabilization of Meisenheimer complex as the reaction intermediate.

The FT-IR spectrum of 4-chloro-2,5-bis-(4′-fluorophenyl)oxazole confirmed the existence of an oxazole ring as shown by a strong absorption band at 1530 $cm^{-1}$ assigned to the –N=C-O- ring stretching frequency. The mass spectrum of this compound contained m/z peaks corresponding to the calculated molecular weights of 292 and 294 with the ratio of 3: 1 due to the presence of chlorine in the molecule. $^{1}H$ and $^{13}C$ NMR data also indicated the structure of 4-chloro-2,5-bis(4′-fluorophenyl)oxazole. In particular, it was clearly revealed by the $^{13}C$ signals at 160.8 (C2), 150.9 (C4) and 138.5 (C5) ppm which are the characteristic $^{13}C$ pattern for 4-chloro-2,5-bis-(4-fluorophenyl)oxazole. The ring formation has been proposed to occur via the formation of acylimidoyl chloride and then reacted further with the carbonyl carbon of the aldehyde. Apparently, 4-chloro-2,5-bis(4′-fluoro phenyl)oxazole can successfully be synthesized in one step with a simple work-up. It should be noted that the fluorine of 4-fluorobenzaldehyde served as the electron donating group in this reaction which retarded the ring formation. That is the reason why, the reaction afforded only 44% yield.

## 4.8. Condensation Polymerization

Much emphasis is placed today on the synthesis of poly(aryl ether)s. The aryl-ether linkage imparts properties such as better solution and melt-processing characteristics and improved toughness compared to the one without aryl-ether linkage. Therefore, this research designs to prepare poly(aryl ether) containing 4-chloro-2,5-diphenyloxazole by condensation polymerization.

### 4.8.1 Characterization

To demonstrate the reactivity of 4-chloro-2,5-bis(4′-fluorophenyl)oxazole monomer for a typical nucleophilic aromatic substitution reaction, a model reaction with phenol was preformed. Both fluoro groups at para positions are easily replaced by phenoxide as a result of activation by the oxazole. A model reaction of monomer with two equivalents of phenol provided very high yield of the substitution product in a typical aromatic substitution reaction condition, suggesting not only high reactivity of this monomer for the nucleophilic displacement reaction, but also the feasibility of the polymer formation in this system. All spectroscopic data from FT-IR and $^{1}$H NMR spectroscopy support the structures of 4-chloro-2,5-bis-(4′-phenoxyphenyl)-oxazole. The FT-IR spectra of this compound show the aryl ether linkage (1150-1250 $cm^{-1}$) and do not show any signals corresponding to the terminal –OH or –F groups, indicating a high conversion.

An oxazole-substituented benzene ring can facilitate nucleophile aromatic substitution by following reasons. First, the electron-poor oxazole ring would act as an electron-withdrawing substituent, and second, the oxazole heterocycle can stabilize the negative charge developed through a stabilized transition state during the transformation to lower the activation energy for the process.

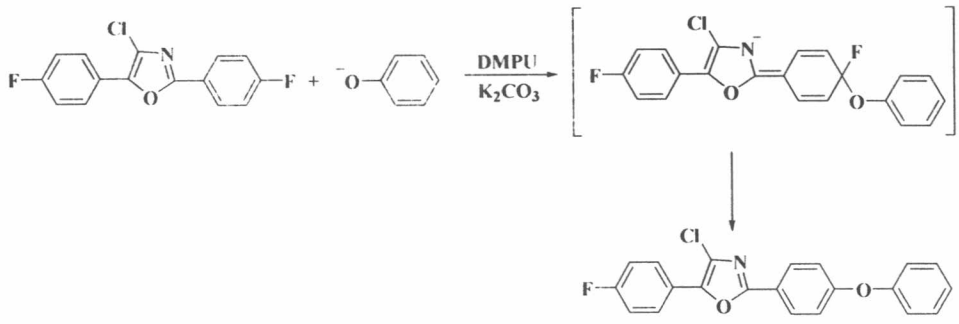


**Scheme 4.12:** Nucleoplilic aromatic substitution

Polymerization of the 4-chloro-2,5-bis(4′-fluorophenyl)oxazole [33] with stoichiometric amounts of bisphenol A was carried out in the presence of potassium carbonate in DMPU/toluene. During the initial stage of the polymerization, the reaction temperature was maintained at 180-200°C to convert bisphenol A to its salt. The reaction was drived by the removal of water from the reaction mixture as the azeotropic mixture with toluene via a Dean-Strak trap. Upon completion of the salt formation and dehydration, the reaction temperature was raised to 220°C to effect the nucleophilic displacement. The influence of polymerization time on molecular weight of the polymer was studied at 3h [CP3], 6h [CP6], 9h [CP9] and 12h [CP12]. After product purification, the occurred polymerization was easily monitored by $^1$H-NMR, by checking the chemical shifts at 6.98, 6.89 and 1.63 belonging to aromatic protons and methyl protons of bisphenol A, respectively. The reaction seems to proceed quite clean at mild reaction condition in DMPU. The desired disubstituted product was obtained with high reaction yield. FT-IR showed a strong absorption band at 1250 cm$^{-1}$, characteristic of the aromatic ether linkage. $^1$H NMR spectrum also showed each aromatic protons and methyl protons with correct integration ratios.

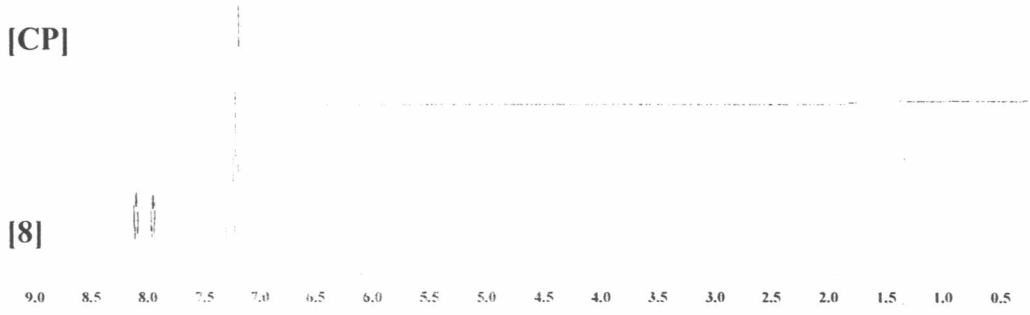


**Figure 4.8:** $^1$H-NMR spectra of 4-chloro-2,5-bis(4′-fluorophenyl)oxazole monomer **[8]** and its condensation polymer **[CP]**

### 4.8.2 Determination of molecular weight

At low reaction time, the low molecular weight of the polymer was obtained as shown in **Table 4.9**.

**Table 4.9:** Polymerization results at different reaction times

| Polymer | Reaction time (h.) | *Mw* |
|---|---|---|
| [CP3] | 3 | 13,844 |
| [CP6] | 6 | 17,295 |
| [CP9] | 9 | 28,118 |
| [CP12] | 12 | 17,115 |

This was presumably due to the lack of sufficient time necessary to maximize the chain growth. At polymerization time greater than 9 h, however, the decrease in molecular weight was resulted. It was probably caused by three possible chain scissions, the attack of KF and the carbonate from base at the polymer chains and transetherification [34]. Similar results on condensation polymerization of the other aromatic difluoride with phenoxides have been reported.

### 4.8.3 Determination of thermal properties

The poly(aryl ether)s exhibit excellent thermal stability as summarized in **Table 4.10**. These polymers showed a 5% weight loss at the temperature ranging from 334 to 363°C as determined by TGA. Maier et al. reported that similar poly(aryl ether oxazole) without a chlorine group on an oxazole unit exhibited decomposition temperatures at 466 °C in nitrogen atmosphere [35]. The source of the instability of the oxazole ring in the polymers can be found by studying the synthetic routes of oxazoles.

**Table 4.10:** Thermal properties of condensation polymers at different reaction times

| Reaction time (h.) | *Tg* (°C) | *Td* (°C) |
|---|---|---|
| [CP3] | 192 | 341 |
| [CP6] | 198 | 344 |
| [CP9] | 205 | 364 |
| [CP12] | 197 | 359 |

Cycloaddition reactions are known to be reversible at high temperatures and therefore oxazoles may be subjected of decomposition to benzonitrile and ketonecarbene. From **Scheme 4.13**, one of the two most important mesomeric structures of the ketocarbene is strongly stabilized by chlorine. Therefore, the activation energy for the cycloreversion of the chlorinated oxazole is lower than that for the cycloreversion of the unsubstituted oxazole, and hence the decomposition of the chlorinated oxazole starts at lower temperatures.

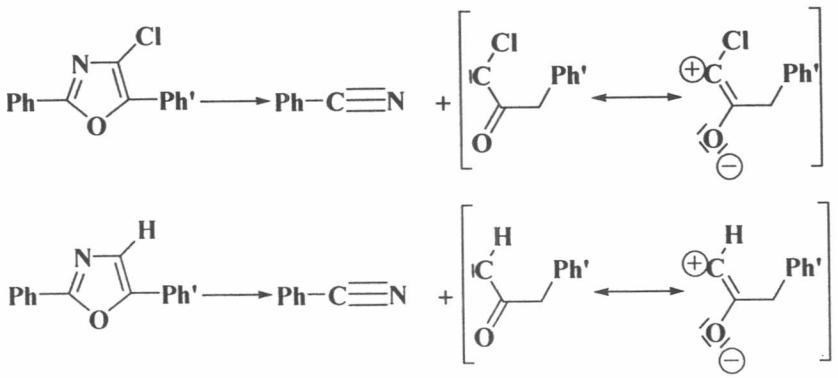


ketonecarbene

**Scheme 4.13:** Decomposition reaction of 2,5-diphenyloxazole

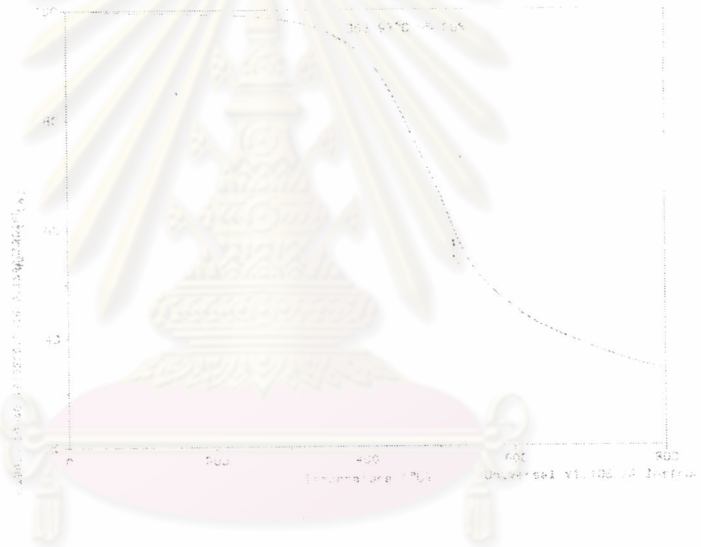

**Figure 4.9:** Typical thermogravimetric curve of condensation polymer in $N_2$

The poly(aryl ether) containing 4-chloro-2,5-diphenyloxazole proved to be amorphous in DSC measurements because the bulky Cl unit in the polymer backbone prevent crystallization. It should be noted that *Tg* depends on molecular weight. High molecular weight results in the high *Tg*.

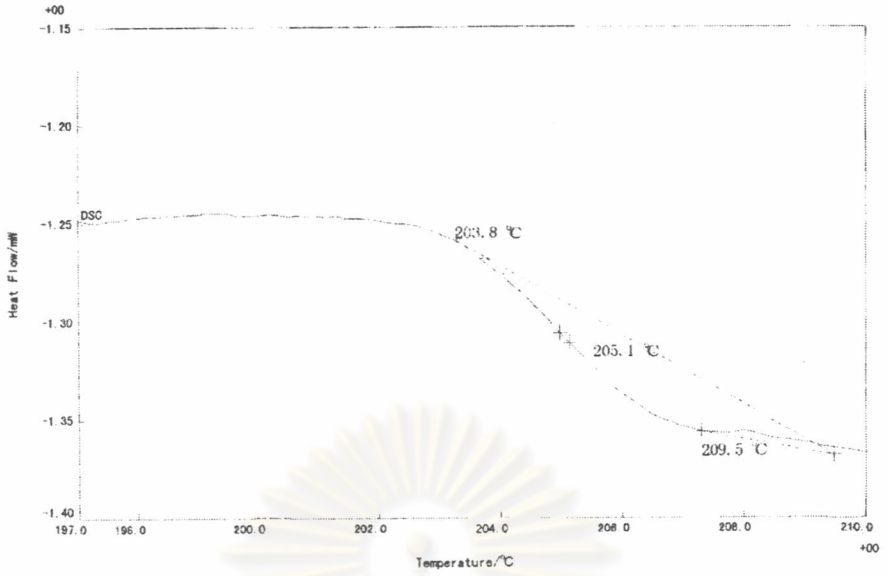


**Figure 4.10:** Typical DSC thermogram of condensation polymer

### 4.8.4 Polymer solubility

The poly(aryl ether) containing 4-chloro-2,5-diphenyloxazole show good solubility in a number of common organic solvents. It was soluble in polar solvents such as NMP, DMPU, and THF at room temperature. The good solubility of these oxazole-containing polymers is in marked contrast to the behavior of other analogue polymers with five-membered heteroaromatic rings. For example, polymers with thiazole groups are soluble in NMP at room temperature but insoluble in THF, even on heating. The thiazole rings result in more extended geometry of the repeating unit. As a result, the backbones of the thiazole polymers are less flexible than those of oxazole polymers.

**Part C: Optical properties**

## 4.9 Optical properties of 4-chloro-2,5-diphenyloxazole derivatives

2,5-Diphenyloxazole, a parent molecule, normally shows a strong maximum absorption at 305 nm, a maximum emission at 376 nm and fluorescent quantum yield of 0.18. The characteristic absorption spectrum of 2,5-diphenyloxazole consists of two absorption bands depending upon the nature of the phenyl substituents at 315-360 nm ($\varepsilon_{max} > 10^3$), and 260-299 nm ($\varepsilon_{max} < 10^3$), respectively. The low-energy absorption is attributed to extended conjugation via the resonance structure while the high-energy absorption is due to $\pi$-$\pi^*$ transition[12].

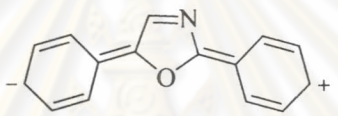


**Figure 4.11:** Extended conjugation via the resonance structure of 2,5-diphenyloxazole

The effect of functional substituents on the spectral characteristics and luminescence intensity of 4-chloro-2,5-diphenyloxazole derivatives has been studied according to the Lambert Beer's law and compared to the 2,5-diphenyloxazole spectral data. The absorption and emission maxima, extrinction coefficient and fluorescence quantum yields are given in **Table 4.11**.

**Table 4.11:** Optical properties of 2,5-diphenyloxazole derivatives

| Compound | $\lambda_{abs}$ [(a)] (nm) | Log ε | $\lambda_{em}$ [(a)] (nm) | $\phi_f$ [(b)] |
|---|---|---|---|---|
| PPO | 305 | 4.58 | 361 | 0.18 |
| [5a] | 351 | 4.45 | 426 | 0.46 |
| [5b] | 346 | 4.29 | 430 | 0.31 |
| [5c] | 360 | 4.61 | 462 | 0.23 |
| [5d] | 363 | 4.37 | 426 | 0.04 |
| [8] | 264 | 4.20 | 369 | 0 |
| [6a] | 311 | 4.56 | 370 | 0.12 |
| [6b] | 311 | 4.47 | 371 | 0.12 |
| [6c] | 321 | 4.66 | 393 | 0.13 |
| [6d] | 358 | 4.44 | 402 | 0 |
| [7a] | 311 | 4.49 | 375 | 0.10 |
| [7b] | 311 | 4.46 | 377 | 0 |
| [7c] | 324 | 4.47 | 400 | 0.37 |
| [7d] | 356 | 4.46 | 425 | 0.02 |
| [7e] | 352 | 4.21 | 456 | 0.27 |

[(a)] Solvent tetrahydrofuran, $c = 1x10^{-5}$ mol/L for absorption measurements, $c = 1x10^{-8}$ mol/L for emission measurements. - [(b)] External standard was anthracene.

### 4.9.1 Absorption spectra

The absorption spectra of 4-chloro-2,5-diphenyloxazole derivatives were measured in THF at the concentration of $1x10^{-5}$ M. Compared to parent 2,5-diphenyloxazole (PPO), the absorption maximum of 4-(4′-chloro-5′-phenyloxazol-2′-yl)benzaldehyde **[5a]** showed a distinct bathochromic shift ($\Delta\lambda_{abs}$= +50 nm). The nearly unaltered shape of the absorption bands implied that the absorption peak is caused by same contribution of vibronic states. It is well known that substituents can affect the spectral data through resonance and field effects. Electron donating substituents led to a bathochromic shift of the absorption maximum while electron withdrawing groups show the opposite effect. It is therefore not surprising that introduction of methoxy group **[5c]** caused a bathochromic shift of the absorption

maximum ($\Delta\lambda_{abs}$= +10 nm) compared to **[5a]**. However, 4-[4′-chloro-5′-(4-fluorophenyl)oxazol-2′-yl]benzaldehyde **[5b]** caused an opposite hypsochromic shift ($\Delta\lambda_{abs}$= -5 nm). The effect of extending the conjugated π-system is seen in 4-[4′-chloro-5′-(4-nitrophenyl)oxazol-2′-yl]-benzaldehyde **[5d]** ($\Delta\lambda_{abs}$= +12 nm). When the hydrogen atoms at the para position of 4-chloro-2,5-diphenyloxazole were replaced by fluorine atoms, as represented in **[8]**, a distinct blue shift of the absorption maximum ($\Delta\lambda_{abs}$= -36 nm) occurred.

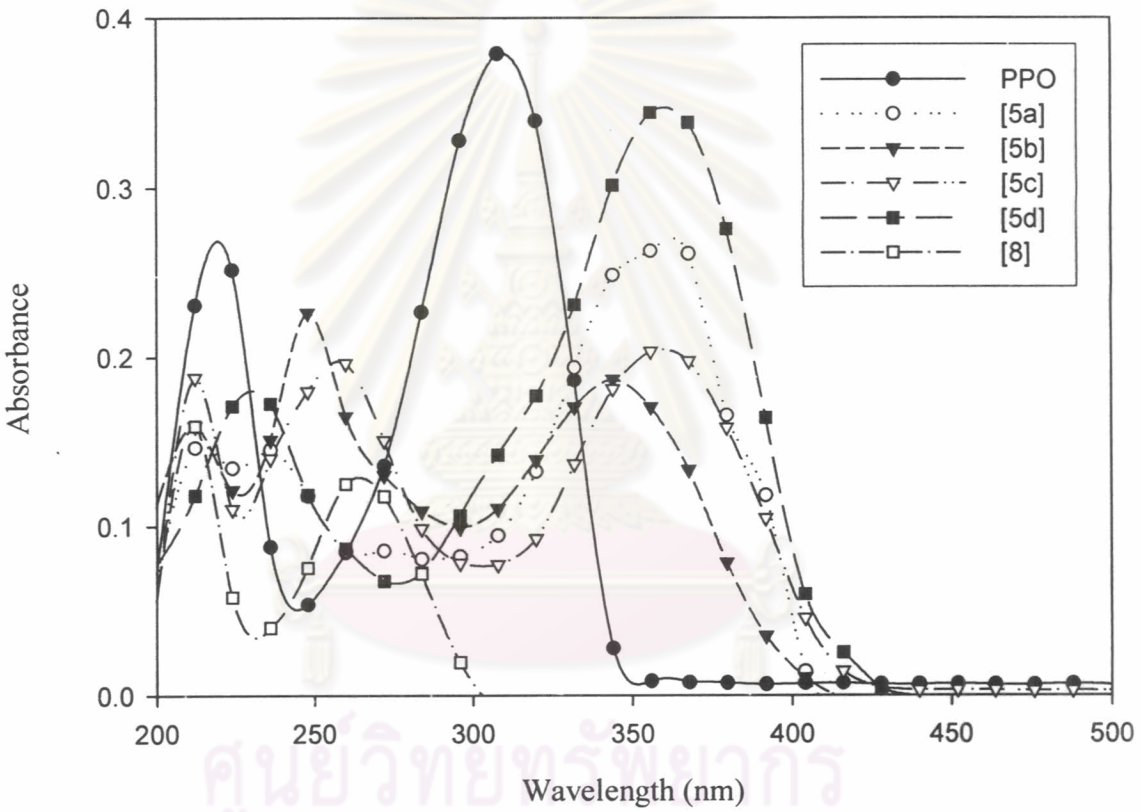


**Figure 4.12:** Absorption spectra of compound **[5a-d]**, **[8]** and PPO in $1x10^{-5}$M

The expected hypsochromic shift occurs ($\Delta\lambda_{abs}$= -40 nm) when the formyl group **[5a]** was replaced by hydroxyl group **[6a]**, as shown in **Figure 4.13**. Since the formyl group at para position of phenyl extends the conjugation length.

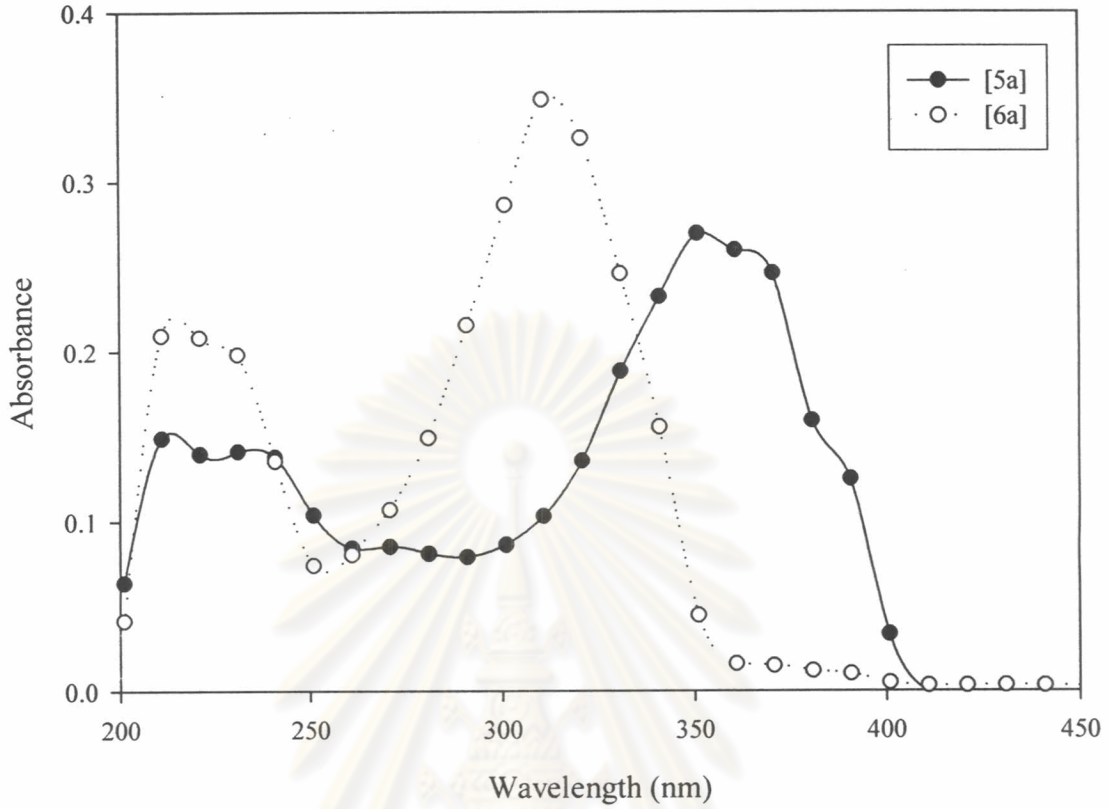


**Figure 4.13:** Absorption spectra of compound **[5a]** and **[6a]** in $1x10^{-5}$M

The same trend of substitution effect was observed for **[6a-d]**, as represented in **Figure 4.14**. The significant bathochromic shifts ($\Delta\lambda_{abs}$= +10 nm) and ($\Delta\lambda_{abs}$= +47 nm) were found in {4-[4′-chloro-5′-(4-methoxyphenyl)oxazol-2′-yl]-phenyl}methanol **[6c]** and {4-[4′-chloro-5′-(4-nitrophenyl)oxazol-2′-yl]-phenyl}methanol **[6d]**, respectively.

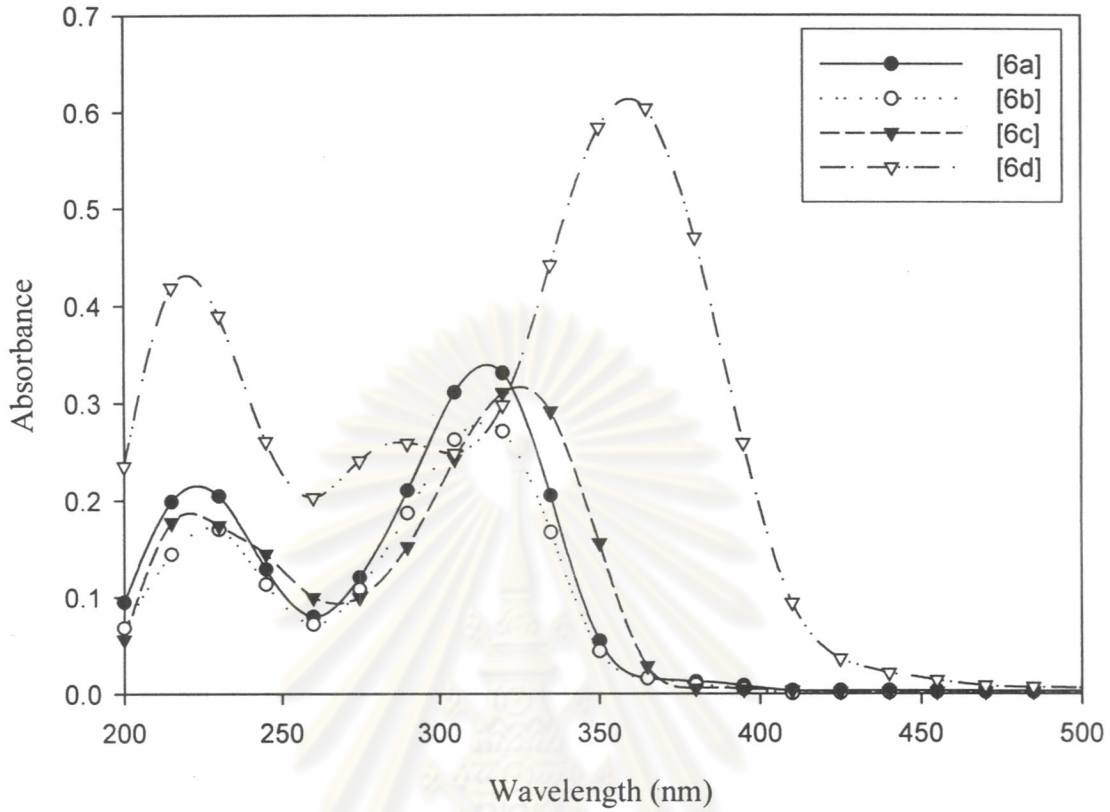


**Figure 4.14:** Absorption spectra of [4-(4′-chloro-5′-phenyloxazol-2′-yl)phenyl] methanol derivatives $1x10^{-5}$ M in THF

Acrylic monomers, **[7a-d]** absorb at $\lambda_{max}$ 311, 311, 324 and 356 as shown in **Figure 4.15**, respectively, which are corresponding to $\lambda_{max}$ of compounds **[6a-d]**. Since methyl methacrylate did not attach in a manner to increase the conjugation length. Therefore, the absorption peak of [4-(4′-chloro-5′-phenyloxazol-2′-yl)phenyl] methyl methacrylate derivatives are nearly unchanged comparing with [4-(4′-chloro-5′-phenyloxazol-2′-yl)-phenyl]methanol derivatives.

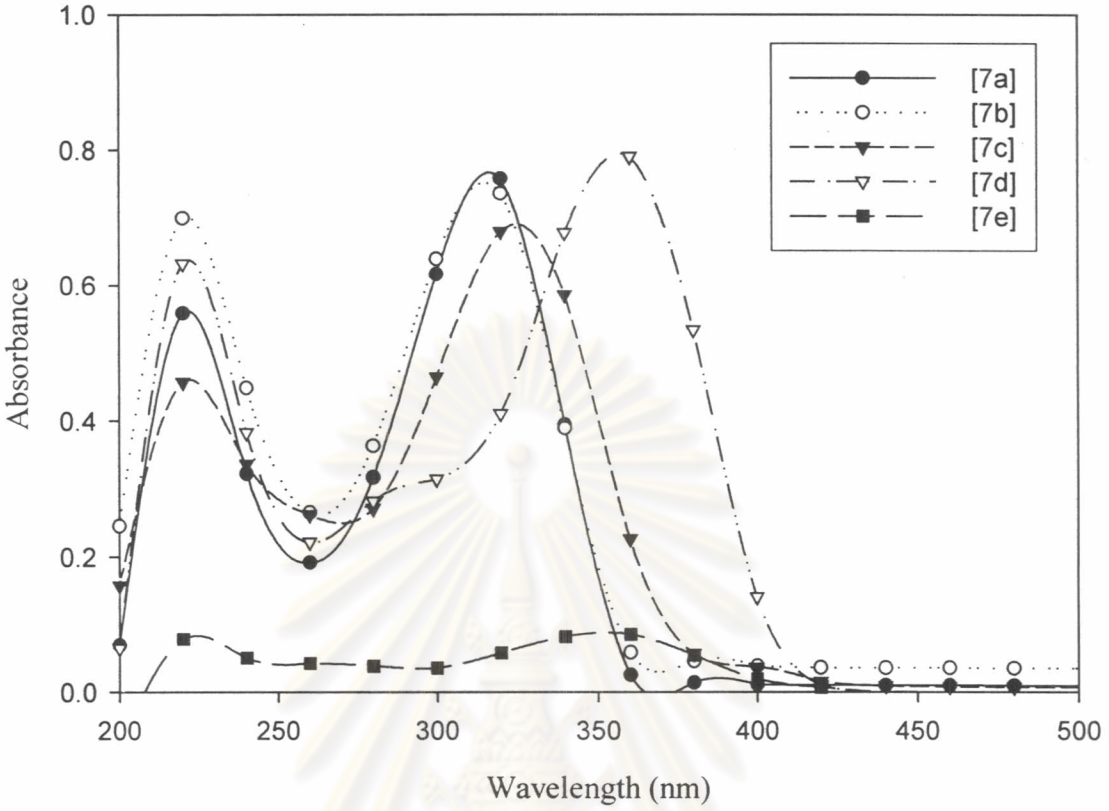


**Figure 4.15:** Absorption spectra of 4-(4′-chloro-5′-phenyloxazol-2′-yl)phenyl]methyl methacrylate derivatives $1x10^{-5}$ M in THF

Differences in the extinction coefficients of the π-π* transitions of 4-chloro-2,5-diphenyloxazole derivatives are small. Nevertheless, the *p*-methoxy-substituent 4-chloro-2,5-diphenyloxazole **[5c]** and **[6c]** seem to guarantee slightly higher transition probabilities than *p*-unsubstituent analogs **[5a]** and **[6a]**, due to the electron-donating effect of methoxy group. However, the transition probability represented by the extinction coefficient of all derivatives remains identical.

### 4.9.2 Emission spectra

The emission spectra of 4-chloro-2,5-diphenyloxazole derivatives were measured in THF at concentration of $1x10^{-8}$ mol/L. Emission spectra show features similar to those of the absorption spectra. Introduction of methoxy and nitro substituents shift the emission maxima to longer wavelengths.

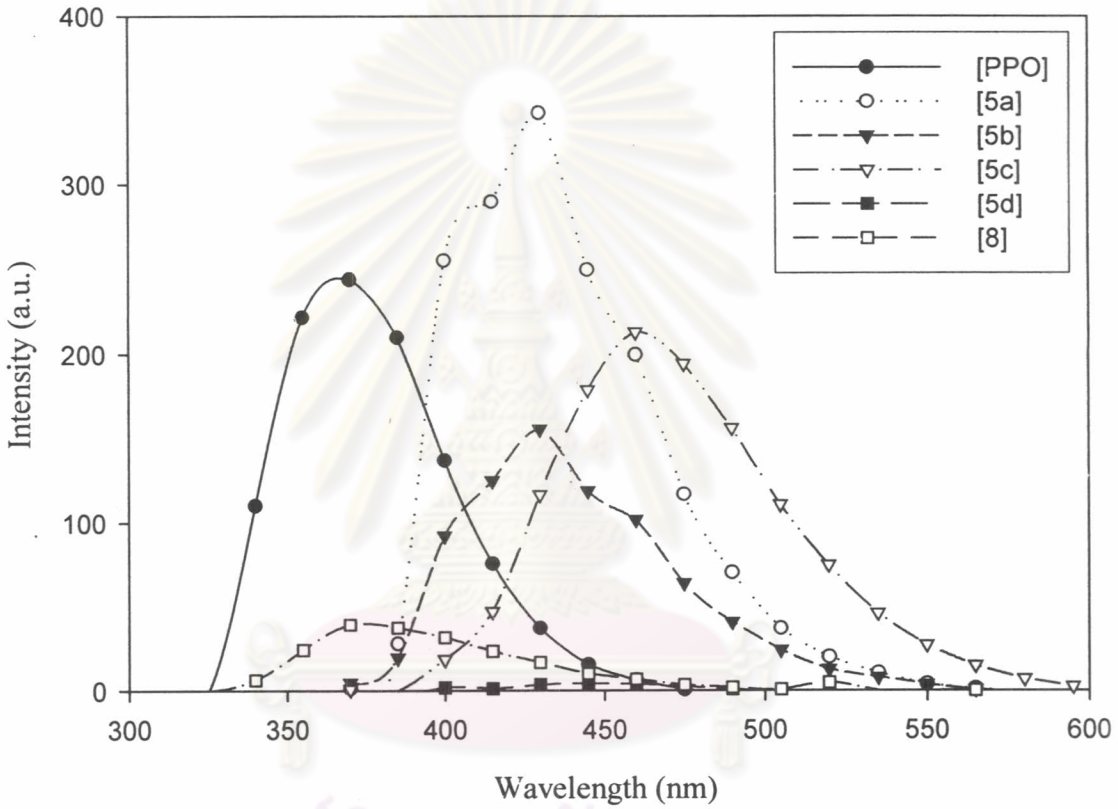


**Figure 4.16:** Emission spectra of compounds PPO, **[5a-d]** and **[8]** at same concentration

The differences in positions of long-wavelength absorption band observed for methoxy and nitro substituents compared to fluoro and unsubstituent are more evident, particularly for the emission spectra of [4-(4′-chloro-5′-phenyloxazol-2′-yl)phenyl] methanol derivatives, **[6a-d]**, and [4-(4′-chloro-5′-phenyloxazol-2′-yl)phenyl] methyl methacrylate derivatives, **[7a-e]**, as shown in **Figure 4.17** and **Figure 4.18**, respectively. It should be noted that at the same concentration nitro substituent emits a lowest intensity comparing with others.

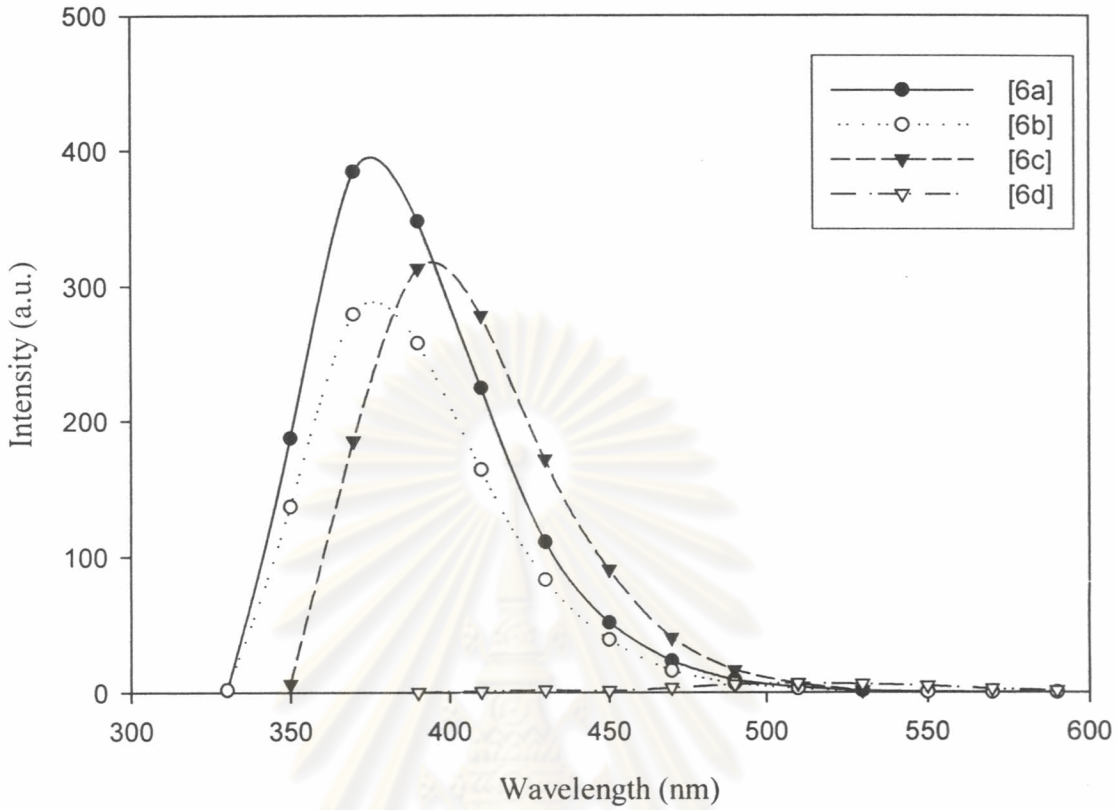


**Figure 4.17:** Emission spectra of compounds **[6a-d]** at $1x10^{-7}M$

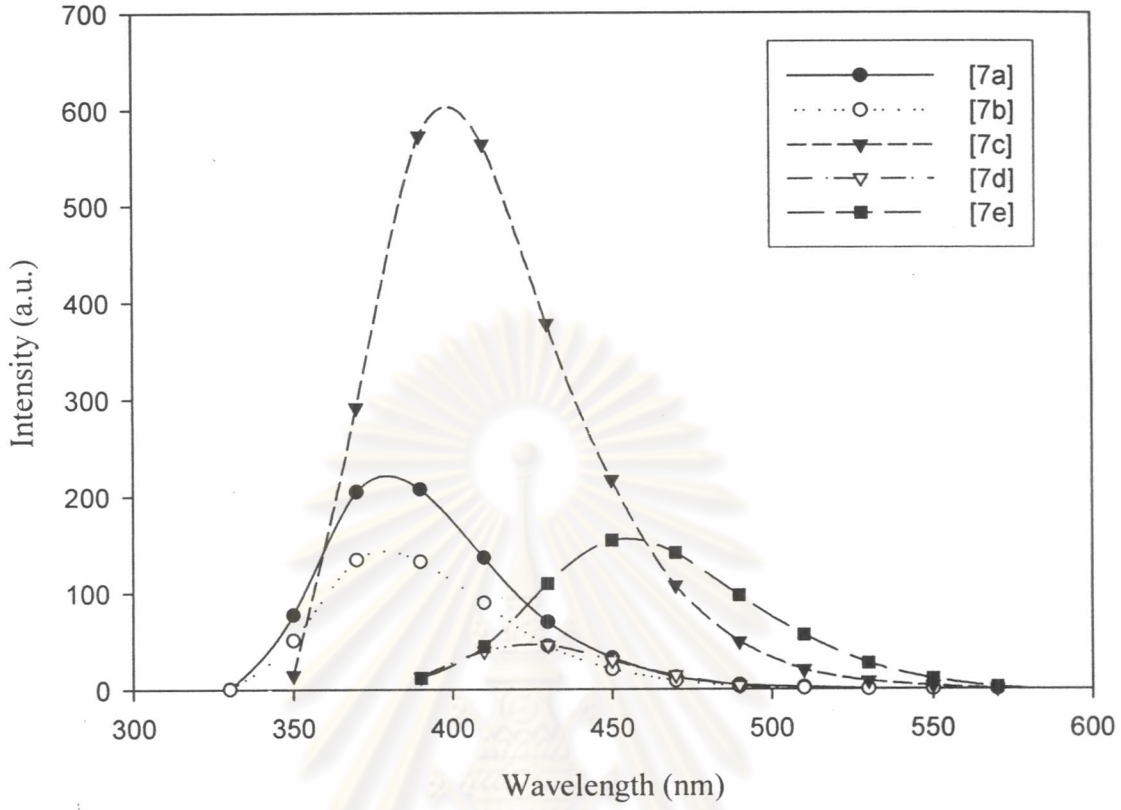


**Figure 4.18:** Emission spectra of compounds **[7a-e]** at $1x10^{-7}M$

Moreover, the compounds were investigated in various concentrations. It was found that the entire compounds in high concentration do not have any excimer emission because they do not show the new emission band in the longer wavelength. When the excimer emission is occurred, a new emission band will be observed in the longer wavelength region.

### 4.9.3 Quantum yield

Some 4-chloro-2,5-diphenyloxazole derivatives investigated in this study show a bright fluorescence in solution, which was quantified in THF at ambient temperature by the optical diluted solution method [27]. Anthracene in ethanol was used as standard. Systematic errors of ± 5% should be taken into account. The introduction of nitro substituent affected the fluorescence quantum yield. The values obtained for 4-[4′-chloro-5′-(4-nitrophenyloxazol-2′-yl]benzaldehyde **[5d]** ($\phi_f$ = 0.04), {4-[4′-chloro-5′-(4-nitrophenyl)oxazol-2′-yl]-phenyl}methanol **[6d]** ($\phi_f$ = 0) and {4-[4′-chloro-5′-(4-nitrophenyl)oxazol-2′-yl]phenyl}methyl methacrylate **[7d]** ($\phi_f$ = 0.02) are somewhat lower than the analogous unsubstituent. Fluorine substituent showed a low fluorescent quantum yield as well, which is more pronounced in 4-chloro-2,5-bis-(4′-fluorophenyl)oxazole, **[8]**. A decrease in fluorescence intensity was found especially in the systems in which a heavy-atom was incorporated in the system as a consequence of heavy-atom effect. Since the probability of nonradiative deactivation processes is promoted by the presence of heavy atoms [36]. Interestingly, the highest fluorescent quantum yield is observed for 4-(4′-chloro-5′-phenyloxazol-2′-yl)-benzaldehyde **[5a]** even the presence of chlorine heavy atom. Low quantum yields can also be explained by classical concentration and color quenching effects, which caused nonradiative decay.

## 4.10 Optical properties of polymers

The absorption and fluorescence spectra of the polymers were studied and compared to the data previously obtained for monomers. The absorption and emission maxima, fluorescence quantum yields and the optical energy gaps are given in **Table 4.12**.

**Table 4.12:** Optical properties of polymers

| Polymer | $\lambda_{abs}$ [(a)] (nm) | Log ε | $\lambda_{em}$ [(a)] (nm) | $\phi_f$ [(b)] |
|---|---|---|---|---|
| [P1] | 313 | 4.96 | 375 | 0.62 |
| [P5] | 318 | 5.21 | 376 | 0.12 |
| [Pf1] | 311 | 4.93 | 378 | 0.13 |
| [Pf5] | 312 | 5.33 | 375 | 0.16 |
| [Pm1] | 325 | 4.59 | 403 | 0.13 |
| [Pm5] | 325 | 5.06 | 401 | 0.13 |
| [Pn1] | 333 | 5.57 | 437 | 0.10 |
| [Pn5] | 334 | 5.64 | 437 | 0.03 |
| [Pnh2] | 335 | 5.12 | 455 | 0.06 |
| [CP] | 321 | 4.50 | 402 | 0.04 |

[(a)] Solvent tetrahydrofuran, $c = 1x10^{-5}$ mol/L for absorption measurements, $c = 1x10^{-8}$ mol/L for emission measurements. - [(b)] External standard was anthracene.

### 4.10.1 Absorption spectra

The absorption spectra of free radical and condensation polymers are shown in **Figures 4.19** and **4.20**, respectively. Reflecting the non-coplanarity and rotational freedom of individual rings, broad and rather nonstructured π-π* transition bands were obtained.

Compared to acrylate monomers, [4-(4′-chloro-5′-phenyloxazol-2′-yl)phenyl] methyl methacrylate derivatives, free radical polymers show an additional absorption peak at 290 nm. This corresponds to the transition of the main chain. The free radical polymers have the similar main chain structures but differ only in the para substitution

of oxazole side chains. Even though the small amount of oxazole moiety was added, the substitution effect was observed, as represented in **Figure 4.19**. The significant bathochromic shifts ($\Delta\lambda_{abs}$= +12 nm) and ($\Delta\lambda_{abs}$= +20 nm) were found in *p*-methoxy substitution **[Pm]** and *p*-nitro substitution **[Pn]**, respectively. The extinction coefficient values of the free radical polymers are significant larger than their monomer analogs. This indicates a higher transition probability of polymers. On account of additional oxazole units, the extinction coefficient value of **[P5]** is significantly larger than **[P1]**, due to the increasing of 4-chloro-2,5-diphenyloxazole chromophore.

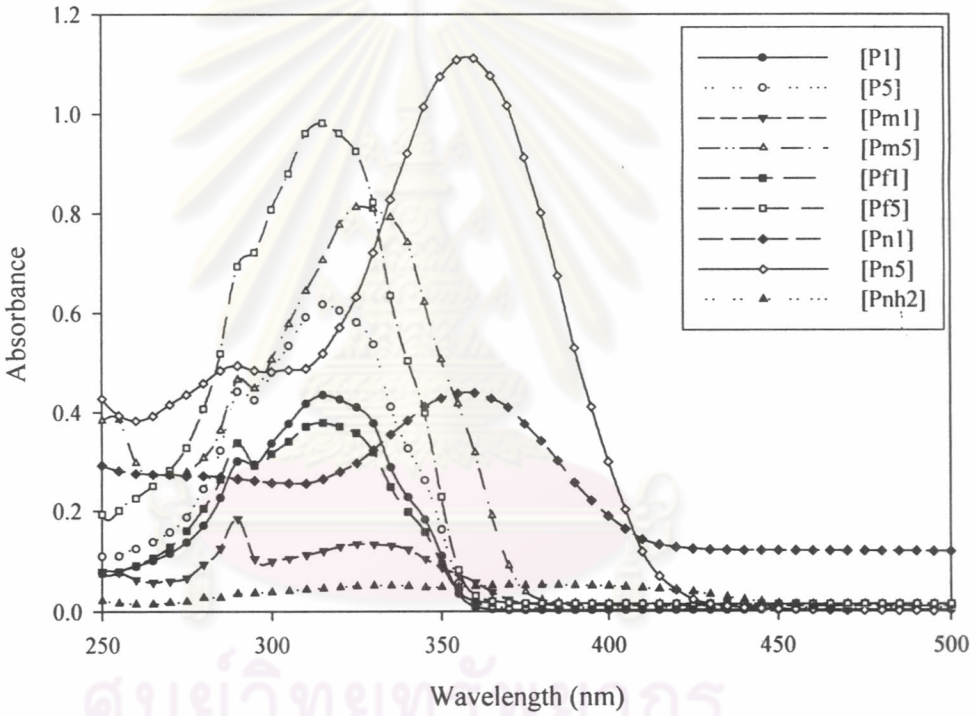


**Figure 4.19:** Absorption spectra of **[P1]-[Pnh2]** at the $1x10^{-5}$M

In the case of 4-chloro-2,5-bis-(4′-fluorophenyl)oxazole and its condensation polymers, the maximum absorption band shifts bathochromically ($\Delta\lambda_{abs}$= +57 nm). The polymer showed the same maximum absorption band as model product. Therefore, the red shift caused by extended conjugation. The nearly unaltered shape of the absorption bands of free radical and condensation polymers suggests that the absorption peak is caused by same contribution of vibronic states of 4-chloro-2,5-diphenyloxazole moiety. Polymers **[CP3]**, **[CP6]** and **[CP12]** were considerably

lower molecular weight than **[CP9]**. Absorption data obtained for the high molecular weight **[CP9]** was virtually identical to its lower molecular weight analogs, as represent in **Figure 4.20**. The extinction coefficient values of the condensation polymers are significant larger than their monomer analogs as well. This confirms the distinctly higher transition probability of polymers.

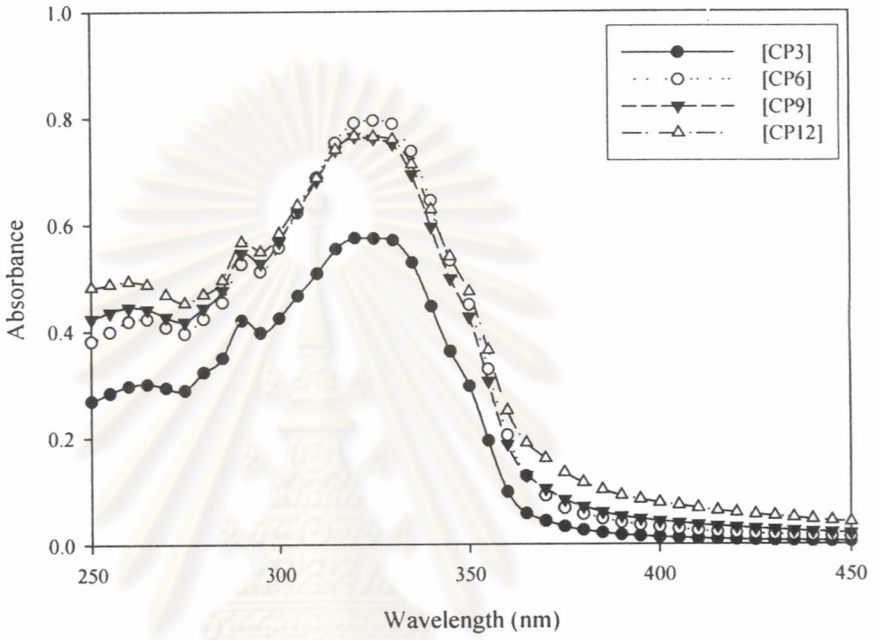


**Figure 4.20:** Absorption spectra of **[CP3]-[CP12]** at the $1x10^{-5}$M

### 4.10.2 Emission spectra

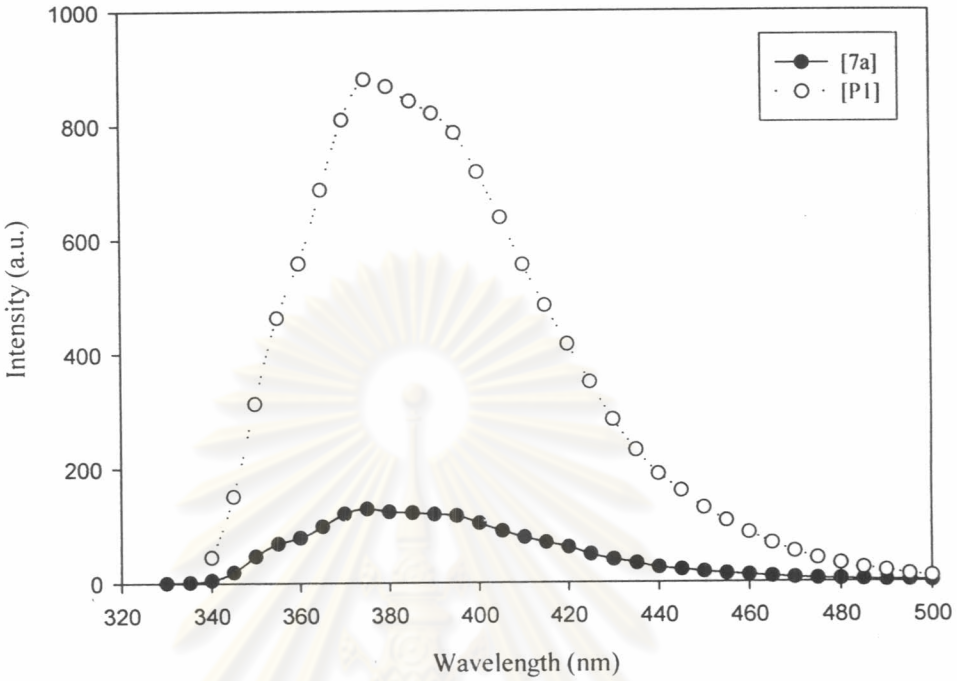


**Figure 4.21:** Fluorescence spectra of **[7a]** and **[P1]** in THF. $\lambda_{ex}$ = 310 nm, Concentration of chromophore = 2.5 x$10^{-7}$ M

Shown in **Figure 4.21** are the emission fluorescence spectra of acrylic monomer and its polymer obtained by excitation at 310 nm (similar results are also obtained for the other five monomers and polymers). Obviously, the polymer exhibited an intense fluorescence at ca. 374 nm, but the monomer displayed very weak fluorescence at the same molar concentration of the chromophore. To confirm that such a low emission fluorescence intensity of the monomer is not caused by concentration factors, the fluorescence emission of the monomers and their polymers at different concentrations were recorded. The fluorescence of **[$P_1$]** is always stronger than that of **[7a]** at any concentration. The 4-chloro-2,5-diphenyloxazole chromophores in monomers may locate in close proximity so that intermolecular interaction may occur and led to fluorescent quenching. On the other hand, it might be difficult for these chromophores to form an interaction in polymers due to the reduced mobility of the pendant chromophores that are attached rigidly to the polymer backbone.

The emission spectra of free radical polymers containing 4-chloro-2,5-diphenyloxazole moiety as a pendent chain were measured in THF. The emission bands of each polymer are more structured than the corresponding absorption bands, indicating more planar and stiffer excited state structure.

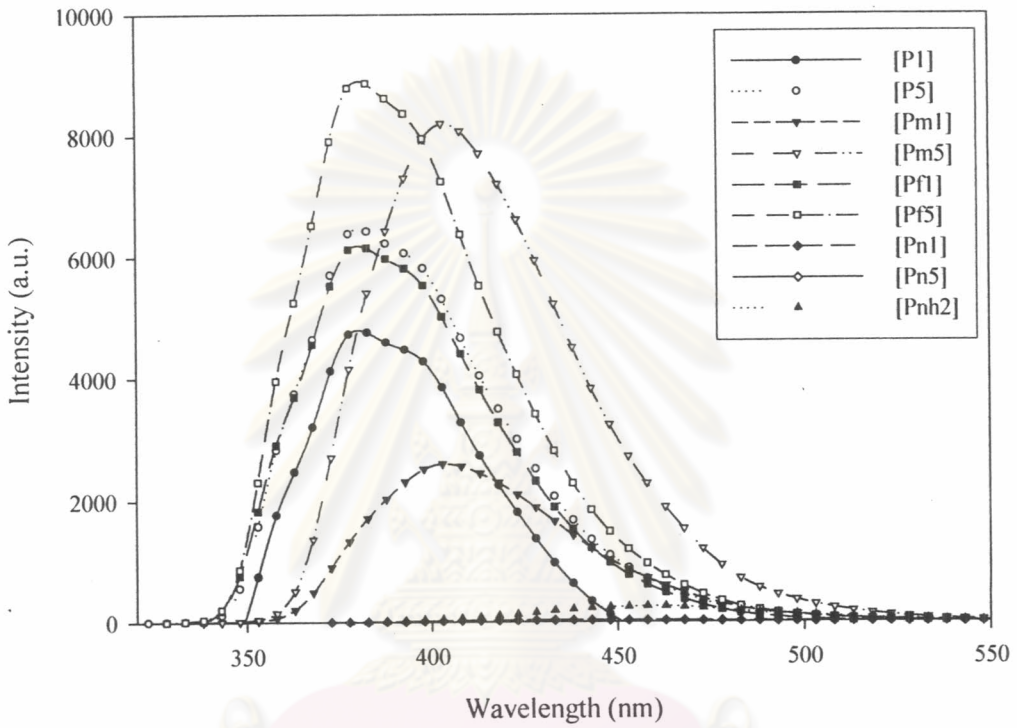


**Figure 4.22:** Emission spectra of **[$P_1$]-[Pnh2]** at the $1x10^{-7}$M

The presence of methoxy and nitro substituents shifts emission maxima to the longer wavelength, due to te hextending conjugated π-system. It is clearly seen that polymer possessing nitro substituents, **[Pn1]** and **[Pn5]**, exhibit a low fluorescent intensity. The fluorescence intensity was more pronouced when the number of 4-chloro-2,5-diphenyloxazole moieties were increased.

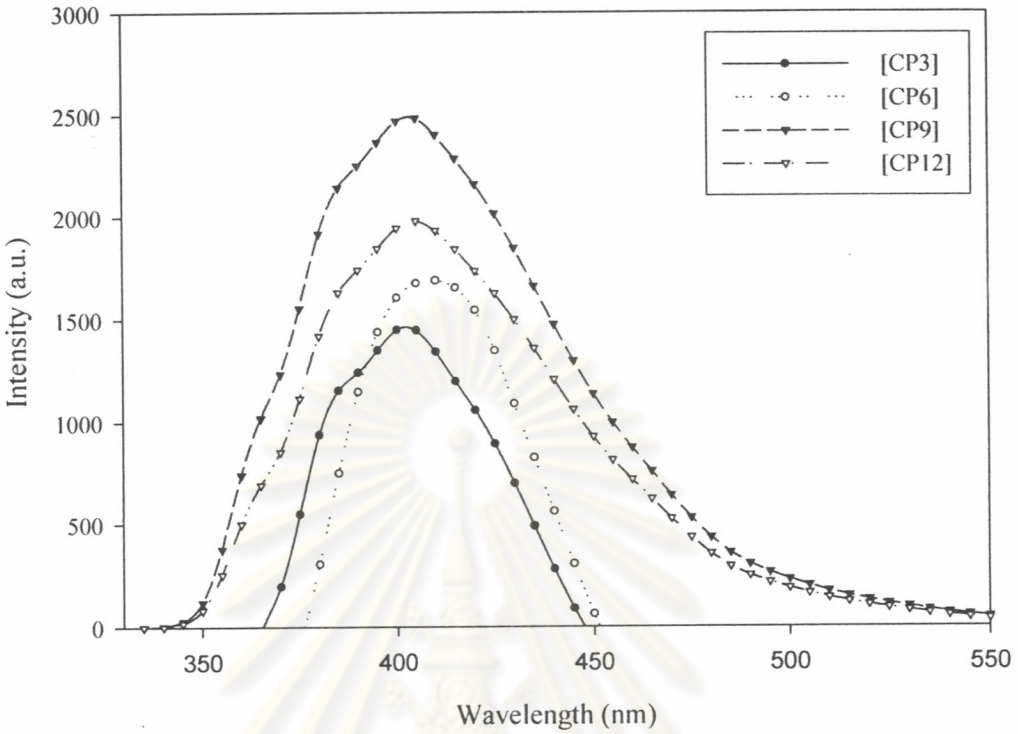


**Figure 4.23:** Emission spectra of **[CP3]-[CP12]** at $1x10^{-7}$M

The emission spectra of condensation polymers containing 4-chloro-2,5-diphenyloxazole moiety in the polymer backbone studied in THF are shown in **Figure 4.23**. Interestingly, the higher molecular weight, the broader emission spectrum was obtained. It should be noted that the highest molecular weight polymer **[CP9]** gave the highest fluorescence intensity.

### 4.10.3 Quantum yield

The highest fluorescence quantum yield is observed for **[P1]**, ($\phi_f$ = 0.62).The 1% feed amount of 4-chloro-2,5-diphenyloxazole chromophore gave a higher fluorescent quantum yield than the 5% feed. The high concentration of 4-chloro-2,5-diphenyloxazole moiety probably quenches the fluorescence resulting in a lower fluorescent quantum yield.

It should be noted that even the presence of 4-chloro-2,5-diphenyloxazole chromophore in the polymer backbone, the fluorescence quantum yield is low. This is possibly due to the helix structure of polymer backbone determined by semi-empirical calculation (**Figure 4.24**).

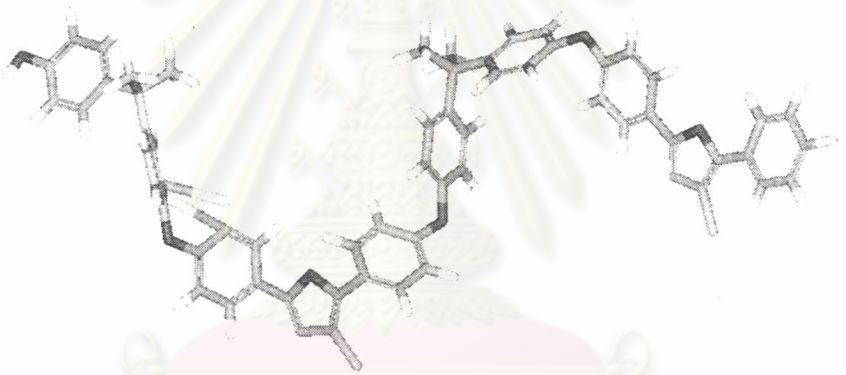

**Figure 4.24:** Calculated optimum structureof tetramer of 4-chloro-2,5-bis-(4′-fluorophenyl)oxazole and bisphenol A

### 4.10.4 Photoluminescence of polymers in solid state

For the photoluminescence of polymers in solid state, thin film of polymers were deposited on quartz substrate. The absorption spectra of the polymer as film are similar to those in solution, and this indicates that their conformation in a solid phase is not greatly changed in comparison with those in a solution phase. However, the emission spectra of thin films of polymers exhibit a relatively very small redshift of 5-8 nm with respect to those in solutions. This is attributed to the disorder of the chain formation caused by the increased coplanarity forced by intermolecular interactions in the solid. The absorption maximum of **[P1]**, both in the solution and in the solid state, is around 310 nm. These similar optical properties seem to indicate that oxazole-based polymers exhibit very similar conformations in both states. Photoluminescence spectra of these polymers show a maximum of emission around 375 nm in solution and 380 nm in solid state. This slight difference might be attributed to weak interchain interactions. These emission spectra show also a vibronic fine structure, generally associated with a rigid and well-defined backbone in the excited state. These polymers do not show any evidence of excimer formation or so-called aggregation emission peak in the solid state and do not seem to lead to the formation of oxidized sites. Photoluminescence of **[Pn1]**, **[Pn5]**, **[Pnh2]** and **[CP]** was not determined due to their poor fluorescence intensity.

**Table 4.13:** Optical properties of polymers in solid state

| Polymer | $\lambda_{abs}$ (nm) | $\lambda_{em}$ (nm) | $\Delta E_{opt}$ (eV) |
|---|---|---|---|
| [P1] | 315 | 378 | 3.35 |
| [P5] | 315 | 382 | 3.40 |
| [Pf1] | 315 | 378 | 3.44 |
| [Pf5] | 315 | 382 | 3.44 |
| [Pm1] | 327 | 403 | 3.31 |
| [Pm5] | 328 | 405 | 3.31 |
| [Pn1] | 353 | - | 2.99 |
| [Pn5] | 359 | - | 2.99 |
| [Pnh2] | 359 | - | 3.10 |
| [CP] | 335 | - | 3.35 |

### 4.10.5 Optical energy gap

The optical energy band gap ($\Delta E_{opt}$) of polymers was calculated from the absorption edge. These results indicate that the polymers are high band gap materials of 2.99-3.44 eV. Although the polymers consisted a small amount of 4-chloro-2,5-diphenyloxazole moiety, band gap and emission maximum of the polymer are similar to those of analogues monomers.

**4.11 Cyclic voltammetry**

In order to investigate the role of 4-chloro-2,5-diphenyloxazole moiety in the polymer, the cyclic voltammetry experiments were preformed, which was used to investigate the redox behavior of the polymer and to assess the HOMO and LUMO energy levels. The potentials were referenced to Ag/AgCl and the reduction potential of ferrocene/ferrocenium in acetonitrile solutions containing 0.1 M of tetrabutyl ammonium tetrafluoroborate ($TBABF_4$) as the supporting electrolyte. The polymer films dip-coated on carbon black electrodes were used as working electrodes and separately scanned anodically and cathodically.

**Table 4.14:** Electrochemical properties and electronic energy levels of the polymers

| Polymer | $E^0_{Red2}$ [(a)] (V) | $E^0_{Red2}$ [(a)] (V) | $E$ (LUMO) [(b)] (eV) | $E$ (HOMO) [(c)] (eV) | $\Delta E_{opt}$ [(d)] (eV) |
|---|---|---|---|---|---|
| [P1] | -2.16 | -1.79 | -3.01 | 0.34 | 3.35 |
| [P5] | -2.16 | -1.72 | -3.08 | 0.32 | 3.40 |
| [Pf1] | -2.18 | -1.86 | -2.94 | 0.50 | 3.44 |
| [Pf5] | -2.18 | -1.80 | -3.00 | 0.44 | 3.44 |
| [Pm1] | -2.26 | -1.82 | -2.98 | 0.33 | 3.31 |
| [Pm5] | -2.24 | -1.82 | -2.98 | 0.33 | 3.31 |
| [Pn1] | -2.28 | -1.85 | -2.95 | 0.04 | 2.99 |
| [Pn5] | -2.30 | -1.85 | -2.95 | 0.04 | 2.99 |
| [Pnh2] | -2.24 | -1.80 | -3.00 | 0.10 | 3.10 |
| [CP] | -2.22 | -2.16 | -2.64 | 0.71 | 3.35 |

[(a)] Reduction onset potential measured by cyclic voltammetry (vs. $Ag/Ag^+$).

[(b)] Calculated from the reduction potentials with absolute level of ferrocene.

[(c)] $E(HOMO) = E_{opt} + E(LUMO)$.

[(d)] Optical band gap derived from the absorption edge of polymer.

In the cathodic scan, the CV of **[P1]** shows two reduction peaks at -1.79 and -2.16 V, respectively. By comparing with the PMMA, it is clear that the reduction peak at -2.16 V of **[P1]** is attributed to the reduction of 4-chloro-2,5-diphenyloxazole moiety in pendent. The rest of the reduction peak at -1.79 V of **[P1]** corresponds to

the reduction of the main chain. The reduction potentials are gradually shifted to higher values due to the electron-withdrawing character of incorporated nitrogen and oxygen atoms. This behavior was obviously revealed by **[Pm1]**, **[Pm5]**, **[Pn1]**, **[Pn5]** and **[Pnh2]**. However, there are no discrete anodic peaks corresponding to p-doping processes. In contrast, the cathodic scans corresponding to n-doping processes show the well-defined and irreversible peaks that make it possible to estimate the values of the lowest occupied molecular orbitals (LUMOs).

All polymers show irreversible redox behavior: a reduction peak appeared during a reductive scan but only a small peak was found in the reverse scan. This suggests that these compounds have an unstable oxidized form under electrochemical conditions. The reduction potential decreases in the order of **[Pn]** > **[Pm]**> **[Pnh2]** > **[Pf]**> unsubstituent polymer. This is the order expected from the nature of the substituents: the ones with withdrawing groups are reduced more readily. As shown in **Table 4.14**, free radical polymer show reduction onset potentials similar to those of condensation polymer, suggesting that electron affinity of the 4-chloro-2,5-diphenyloxazole is greatly affected whether it is incorporated in the backbone or as a pendent group.

The energy levels of the polymers can be estimated from the following equation:

$$LUMO = (-4.8\text{-}E^{0}_{red})eV,$$

Where the –4.8 is the energy level of ferrocene related to vacuum level. In the absence of a direct measurement, of the oxidation potential, the highest occupied molecular orbital (HOMO) energy levels were obtained by the addition of the optical band gap, calculated from the absorption edge of the polymer [37]. The energy levels of the polymer containing 4-chloro-2,5-diphenyloxazole moieties are summarized in **Table 4.14**. These data can be used for the selection of electrode materials in the fabrication of polymer LED.

## 4.12 Fabrication and characterization of LEDs

The current -voltage characteristic of LEDs of acrylate polymer and poly(aryl ether) containing 4-chloro-2,5-diphenyloxazole moieties are determined. Acrylate polymer did not show any addition signal comparing to electrode due to an insulator backbone.

For poly(aryl ether), the turn-on voltage of the diode is ca. 2 V, but the low current densities could be a result of poor charge carrier balance, given the irreversible reduction and lack of oxidation in the CV. No measurable EL could be seen till applied bias of 6 V. Further investigations are in progress to measure and improve these devices.

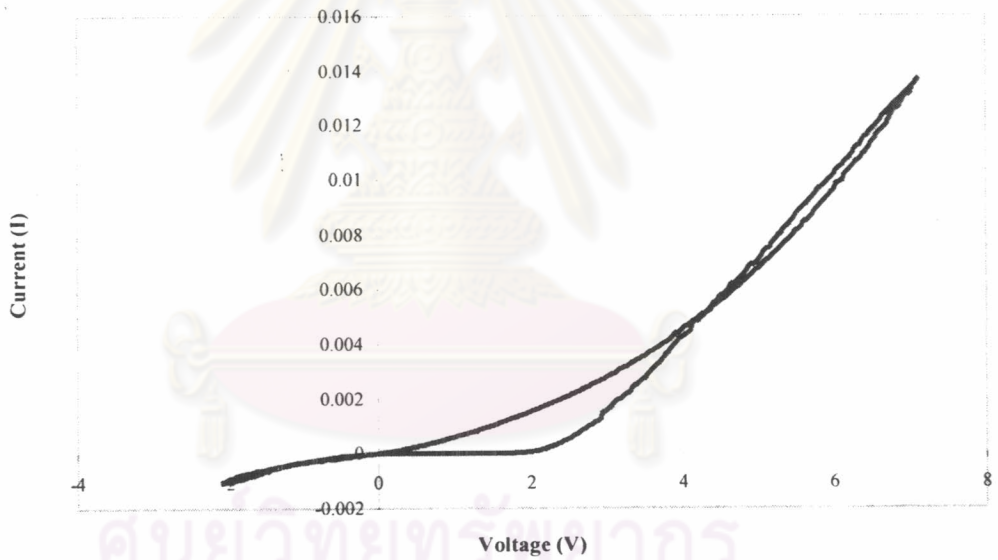


**Figure 4.25**: I-V curve of Poly(aryl ether) oxazole **[CP]**

**Part D: Scintillation efficiency**

## 4.13 Scintillation efficiencies of 4-chloro-2,5-diphenyloxazole derivatives

Functionalized 4-chloro-2,5-diphenyloxazoles were evaluated for the ability to scintillate in the presence of ionizing radiation. The radioactive decay of $^{36}Cl$ produces $\beta$-particles. In $\beta$-particle scintillation counters, the kinetic energy from the radiating particle is absorbed by scintillator molecules, which then relax via fluorescence emission of radiation. The resultant photons can be measured by a photomultiplier tube. The signal in count per minute (cpm) depends on the number of $\beta$-particles that are launched into the scintillator per minute that have sufficient residual energy to produce a photon burst that registers above the threshold level set on the amplifier/discriminator.

$$_{17}Cl^{36} \longrightarrow {}_{18}Ar^{36} + \beta$$

The signal of 2,5-diphenyloxazole, standard scintillator, depends on concentration, as shown below. The plot exhibited an exponential relationship. The signal was more pronouced when the concentration of 2,5-diphenyloxazole was increased. However, the precipitation and non-homogeneous were found at higher concentration. This study designs to setup the experimental condition at 0.25 M.

**Table 4.15:** Scintillation efficiency of 2,5-diphenyloxazole at different concentrations

| Concentration (M) | Counts per minute (cpm) | Counts per second (cps) |
|---|---|---|
| 0.05 | 0 | 0 |
| 0.10 | 9 | 0.037 |
| 0.25 | 4158 | 17.325 |
| 0.50 | 65683 | 273.680 |
| 0.75 | 223287 | 960.362 |
| 1.00 | 594874 | 2478.641 |

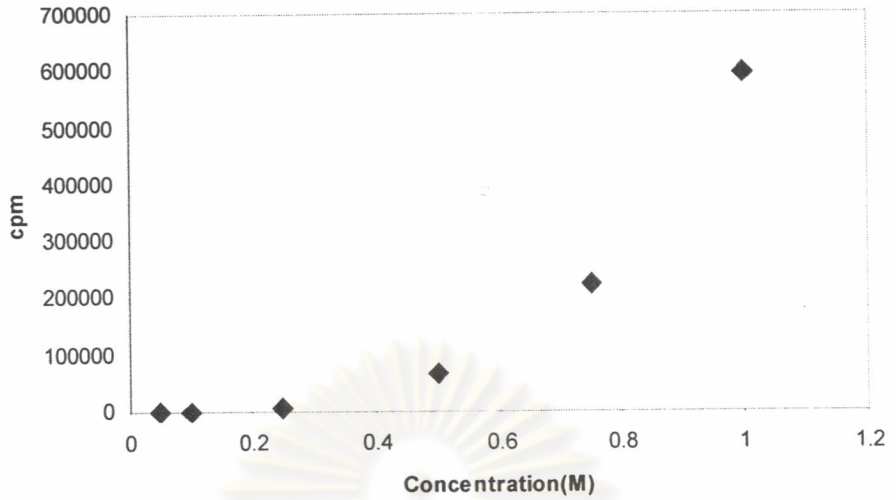


**Figure 4.26:** Count per minute versus concentration of 2,5-diphenyloxazole

**Table 4.16:** Scintillation efficiencies of 2,5-diphenyloxazole derivatives at 0.25 M

| Compound | cpm | cps | % Efficiency at 0.25 M relative to PPO |
|---|---|---|---|
| Cl-PPO | 10 | 0.041 | 0.236 |
| [5a] | 2871 | 11.962 | 69 |
| [5b] | 0 | 0 | 0 |
| [5c] | 0 | 0 | 0 |
| [5d] | 0 | 0 | 0 |
| [8] | 0 | 0 | 0 |
| [6a] | 0 | 0 | 0 |
| [6b] | 0 | 0 | 0 |
| [6c] | 0 | 0 | 0 |
| [6d] | 0 | 0 | 0 |
| [7a] | 104413 | 435.054 | 2511 |
| [7b] | 0 | 0 | 0 |
| [7c] | 0 | 0 | 0 |
| [7d] | 0 | 0 | 0 |
| [7e] | 0 | 0 | 0 |

**Table 4.16** shows that the performance of the functionalized 4-chloro-2,5-diphenyloxazole derivatives as fluor is comparable with 2,5-diphenyloxazole (PPO) itself, which is commercially available. The high efficiency is maintained at the optimum PPO concentration (0.25 M). Compared to 2,5-diphenyloxazole, the scintillating efficiency of 4-chloro-2,5-diphenyloxazole is lower. Since the only structural difference between the two is the chlorine atom. It seems that the scintillating efficiency of 4-chloro-2,5-diphenyloxazole is somehow quenched by chlorine atom. The addition of high Z-elements inevitably lead to a decreased light output. Introducing of formyl group, **[5a]**, lead to a larger scintillating efficiency value comparing to 4-chloro-2,5-diphenyloxazole. This occurs due to the higher fluorescence quantum yield of **[5a]**. While, other substituent, **[5b-d]**, did not give any signal. It is important to point out that color quenching occurs when color compounds are present in the sample and absorb or scatter some of the light [38]. That is the reason why, the counting signal of other color compounds were absent. Although, the fluorescence quantum yield of **[5a]** is higher than PPO, its scintillation efficiency is lower. However, the presence of Cl group in **[5a]** cause a reduction of the count. A possible explanation for the low scintillation efficiency comparing to PPO may be these two effects compose each other and the effect of Cl group plays a dominant role. Surprisingly, the scintillating efficiency is tremendous facilitated with the introduction of methyl methacrylic group, **[7a]**, which is ever higher than PPO. This is presumably due to the closer matching of maximum emission of **[7a]** to the spectral sensitivity of a Li-glass photomultiplier tube (395 nm).

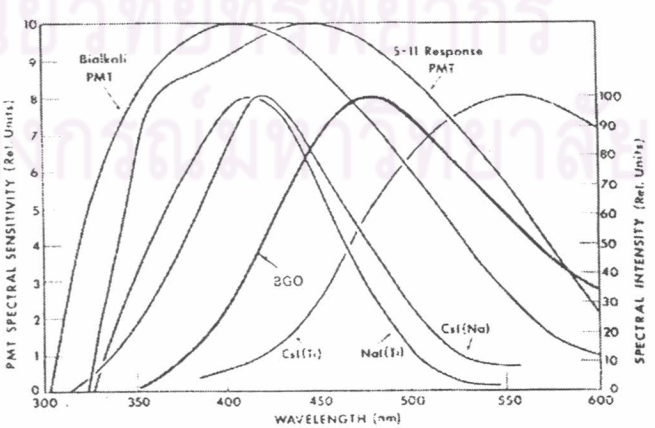


**Figure 4.27:** Response curves for widely use photomultiplier tube (PMT)

Additionally, the presence of bulky group, which interferes with two molecules coming together in the proper orientation for excimer formation, eliminates self-quenching. PPO, undergo self-quenching, have a planar configuration, which is unhindered by the approach of a second molecule. The comparing scintillation counting efficiency of 4-chloro-2,5-diphenyloxazole derivatives are shown below.

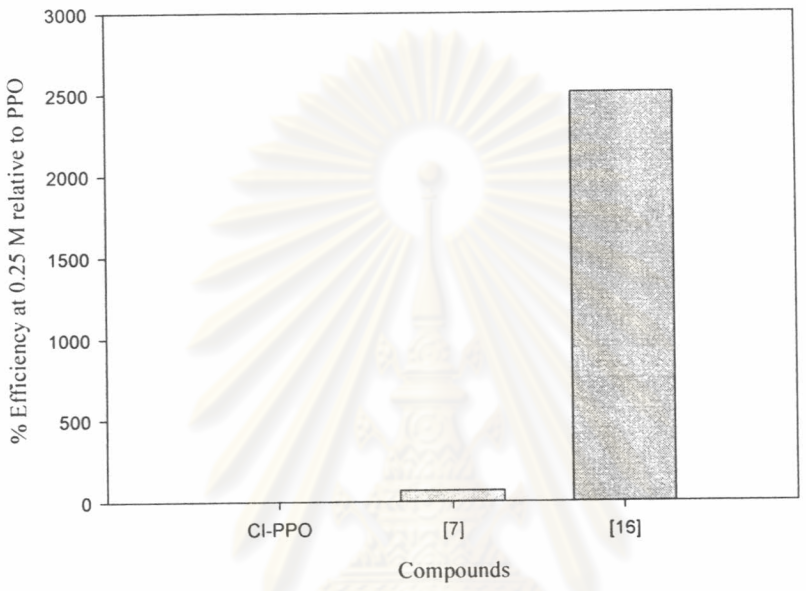


**Figure 4.28:** Scintillation efficiencies of 4-chloro-2,5-diphenyloxazole derivatives

Scintillation efficiencies vary with the size and conformer of scintillate containing molecule, fluorescence quantum yields and with the spectral distribution of the emission in relation to the photomultiplier sensitivity of the scintillation counter.

## 4.14 Scintillation efficiency of polymers containing 4-chloro-2,5-diphenyloxazole derivatives

The scintillation efficiency of polymers containing 4-chloro-2,5-diphenyloxazole derivatives is shown in **Table 3.13**. The maximum scintillation efficiency was found in **[P1]**. Scintillation efficiencies of polymer containing substituent 4-chloro-2,5-diphenyloxazole derivatives were quenched, as expected, due to the color quenching. Comparing with PPO, scintillation counting value was low, largely due to a smaller amount of scintillating unit. However, it should be noted that even 1% of scintillating unit can detect the ionizing radiation. Interesting, scintillation efficiency of **[P5]**, increasing of scintillating unit, turn out a lower result than **[P1]**. A possible explanation for the low scintillation efficiency is due to the lower fluorescence quantum yield of **[P5].** This effect is also proved in condensation polymer **[CP]**. Even though, number of scintillating unit increased, the signal was quenched. Besides, incorporation of 4-chloro-2,5-diphenyloxazole in the polymer backbone presumably led to a poor signal since the catenation angle at the oxazole ring caused helix backbone.

**Table 4.17:** Scintillation efficiencies of polymer containing 2,5-diphenyloxazole derivatives at 0.25 M

| Compound | cpm | cps | % Efficiency at 0.25 M relative to PPO |
|---|---|---|---|
| [P1] | 2250 | 9.37 | 54 |
| [P5] | 440 | 1.83 | 11 |
| [Pf1] | 0 | 0 | 0 |
| [Pf5] | 0 | 0 | 0 |
| [Pm1] | 0 | 0 | 0 |
| [Pm5] | 0 | 0 | 0 |
| [Pn1] | 0 | 0 | 0 |
| [Pn5] | 0 | 0 | 0 |
| [Pnh2] | 0 | 0 | 0 |
| [CP] | 0 | 0 | 0 |

**Part E: Electrospinning**

## 4.15 Electrospinning

To fabricate fluorescent polymer, the electrospun membranes were prepared on glass substrates. The SEM images in **Figures 4.29** and **4.30** were obtained from the electrospun membrane of the polymer **[P1]** with PMMA matrix and PS, respectively. These images show the fibrous structure of the electrospun membrane with a diameter ranging from approximately 1-10 μm, which is typical of electrospun fibers.

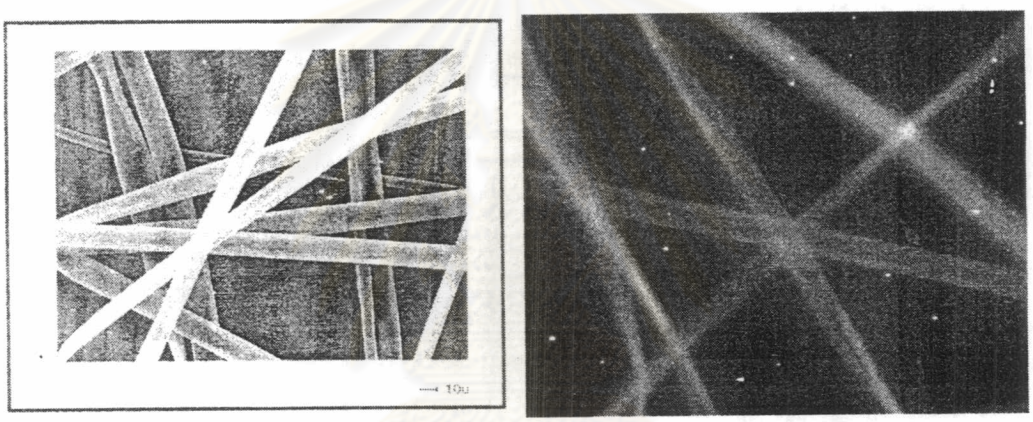

**Figure 4.29:** SEM image of an electrospun membrane of **[P1]** in PMMA matrix

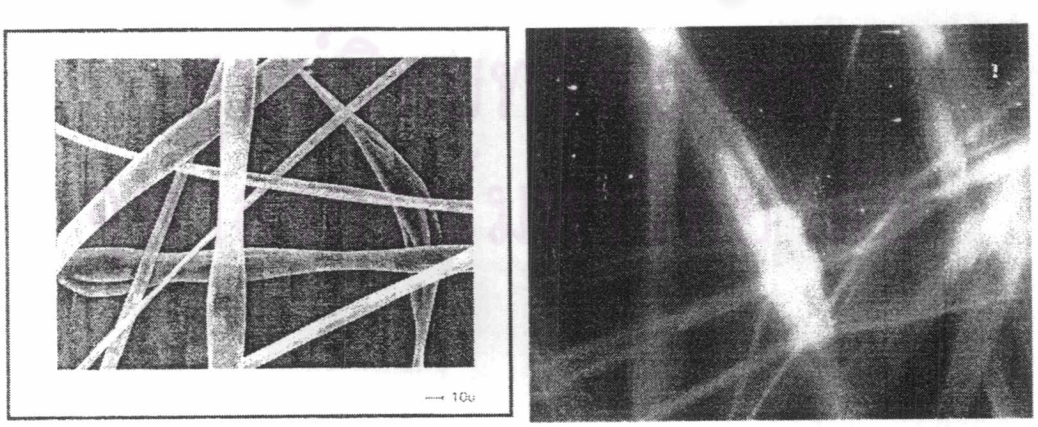

**Figure 4.30:** SEM image of an electrospun membrane of **[P1]** in PS matrix

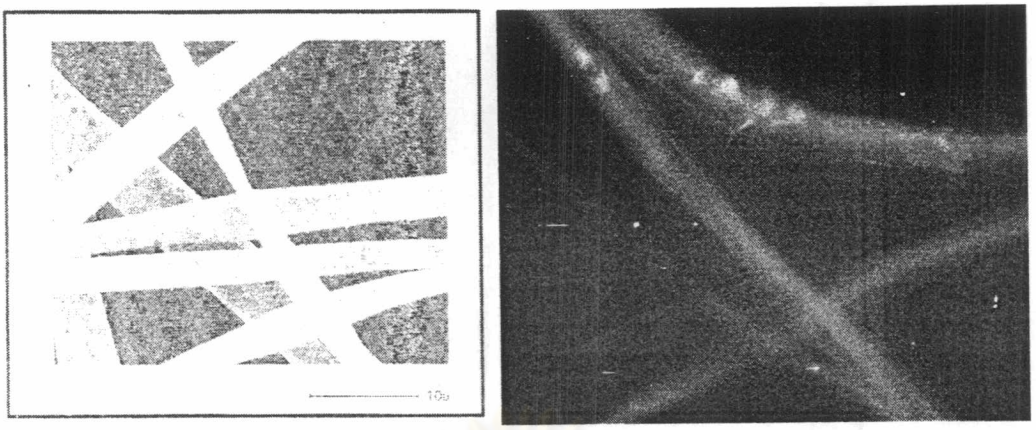

**Figure 4.31:** SEM image of an electrospun membrane of **[Pm1]** in PMMA matrix

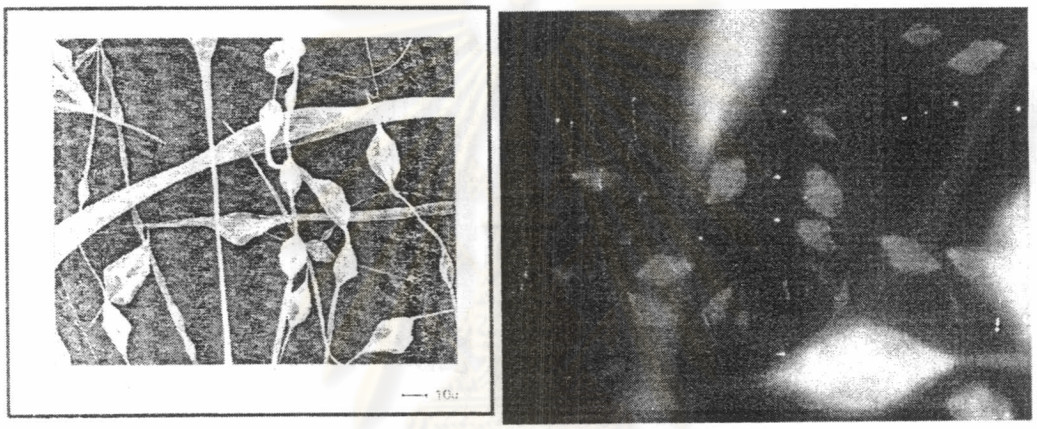

**Figure 4.32:** SEM image of an electrospun membrane of **[Pm1]** in PS matrix

**Figure 4.33:** SEM image of an electrospun membrane of **[CP]** in PS matrix

An interesting feature found in **Figures 4.32** and **4.33** was bead formation along their length. The beads observed have a wrinkled, "raisin"-like surface texture that is different from the smooth ellipsoids, **Figures 4.29**, **4.30** and **4.31**. This is most likely attributable to collapse of the ellipsoids after evaporation of the residual

solvent. The bead morphology has been previously documented for electrospun fibers, and is affected by processing condition. These polymers can be fabricated and used for high throughput screening proposes.

The fluorescence property of the electrospun fibers was analyzed using fluorescent microscopy. The results demonstrate the blue emission of acrylate polymer and poly(aryl ether) oxazole.